

Fusion Simulation Project:

Integrated Simulation & Optimization of Fusion Systems

Final Report of the FESAC ISOFS Subcommittee • December 1, 2002



$$\frac{\partial f_a}{\partial t} + \mathbf{v} \cdot \nabla f_a + \frac{q_a}{m_a} [\mathbf{E} + \mathbf{v} \times \mathbf{B}] \cdot \nabla f_a = C(f_a)$$

FUSION SIMULATION PROJECT (FSP)

Integrated Simulation & Optimization of Fusion Systems

Appendix. Overview of Fusion Science for the FSP

- I. Introduction – Fusion Science Insights and Challenges**
 - A. Insights from numerical simulation
 - B. Simulation challenges
- II. Fusion Science Basic Concepts**
 - A. Basic equations
 - B. Reduced descriptions
- III. Microscopic Simulation**
 - A. Introduction and summary
 - B. Neoclassical transport
 - C. Turbulence and anomalous transport
 - D. Non-local phenomena
 - E. Challenges for turbulence simulation
- IV. Macroscopic Simulation**
 - A. Introduction and summary
 - B. Equations
 - C. Status
 - D. Challenges
- V. Plasma Edge Physics and Plasma-Wall Interaction**
 - A. Introduction
 - B. Properties of the edge plasma
 - C. Computational challenges and codes for the edge region
 - D. Whole Device Modeling
- VI. Equilibrium Evolution and Confinement**
 - A. Introduction
 - B. Transport equations
 - C. Uses of transport codes
 - D. Challenges of transport modeling

- VII. External Sources**
 - A. Introduction
 - B. Neutral beam injection
 - C. Edge particle sources
 - D. Radio-frequency wave heating and current drive
 - E. Summary: the role of source models in comprehensive integrated simulation
- VIII. Fusion Simulation Capabilities Status**
- IX. Focused Integration Initiatives – Challenges and Opportunities**
 - A. Plasma edge
 - B. Turbulence on transport timescales
 - C. Global stability
 - D. Whole device modeling
- X. Validation Requirements in Fusion Topical Areas**
 - A. Transport
 - B. MHD
 - C. Radio-frequency heating and current drive
 - D. Edge/scrape-off-layer/divertor
- XI. Background – Orbits and Instability Mechanisms**
- XII. Glossary**

I. INTRODUCTION — FUSION SCIENCE INSIGHTS AND CHALLENGES

This appendix summarizes the status of fusion science, emphasizing its theoretical and computational aspects. We wish to demonstrate first the scope and complexity of the physics and mathematics, second the progress that has been made up to now, and third the great challenges and opportunities before us. We discuss the several areas of fusion physics and computation that are referred to in the main report, beginning with a brief introduction to the basic equations and concepts in Sec. II. We follow this with more detailed surveys of the main areas of concern in Secs. III-VII. In Sec. VIII we summarize the 50 or so principal codes in use today. In Secs. IX and X we explore the focused integration initiative examples and validation requirements that are introduced in the main body of the report. In Sec. X we give a very brief review of some elementary plasma physics concepts. Finally, in Sec. XI, there is a glossary. Words introduced in *italics* are defined there.

Before going into the various topics, let us begin by examining our ultimate goal from the point of view of past accomplishments in computational plasma physics and some challenges that we expect will lead to future insights.

Numerical simulation and modeling, at varying stages of integration, have contributed greatly to insights regarding the behavior of magnetically confined plasmas. This has resulted from the continual interaction among computation, theory, and experiment. As the Fusion Simulation Project (FSP) develops, and wider ranges of physical processes are integrated into the simulations, there will be greater and greater reliance on massive computations. At the same time, as pointed out in the main text, the theoretical interpretation and experimental validation efforts will continue to be crucial to the overall success of the project.

We present a few examples to illustrate how this process works and how computation has contributed and will contribute to our insight and understanding.

A. INSIGHTS FROM NUMERICAL SIMULATION

1. Global stability and major disruptions in tokamaks

A *major disruption* is the name given to an abrupt abnormal termination of a *tokamak* discharge with total loss of plasma current and confinement. This is thought by many to be the major obstacle that could potentially upset the development path of the tokamak as a practical energy source. Besides terminating the discharge, the disruption has the adverse effects of producing large thermal loads on the *divertor* and large electromagnetic forces on the vessel wall. (See cutaway view in Fig. III.1 of the main report.) Disruptions also have the potential of accelerating electrons to multi-MeV energies, and these can cause additional severe damage to the first wall.

Computer simulations have been crucial in identifying specific sequences of events that can cause disruptions. An excellent example of this are the simulations that explained the major disruption in the record-setting *TFTR* discharge that produced 10 MW of fusion power. [E. Fredrickson, W. Park, et al, “High-beta disruption in tokamaks”, Phys. Rev. Lett, 75 1763 (1995)]. It was shown that under the conditions of that discharge, it was energetically favorable for the plasma

interior to deform into a long-wavelength helical structure. In the local regions of the torus where the *unfavorable curvature* of the helical structure aligned with the curvature of the torus itself, the plasma pressure could very easily cause instability. It was the interaction of this localized *ballooning* instability with the interior long-wavelength helical structure that destroyed the nested *magnetic surfaces* and precipitated the disruption. Figure A1 depicts a simulation of this process, with perturbed field lines and *poloidal* cross sections highlighted in colors representing mode amplitude.

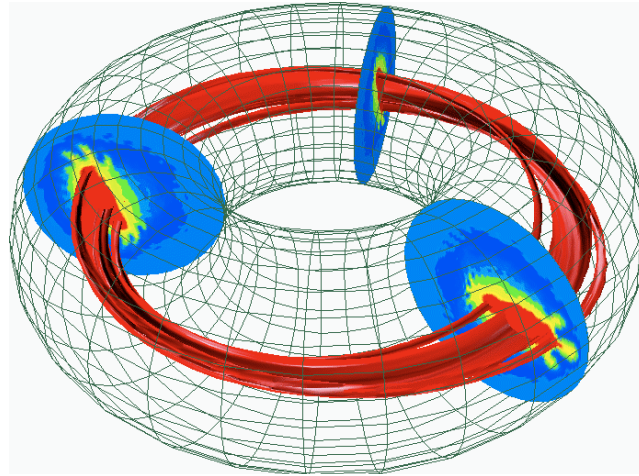


Fig. A1. An internal helical structure interacting with the toroidal geometry causes localized instability that can lead to a major disruption. [Courtesy Wonchull Park, PPPL]

There are other causes of the major disruption, which we are just beginning to understand and are finding ways to control. Integrated simulations of the kind planned in this project will be instrumental in identifying and understanding these mechanisms. (See Sec. IV.)

2. Design of Three Dimensional Toroidal Configurations

Another example with already some degree of integration is the design of three-dimensional (3-D) stellarator configurations. *Stellarators* are advanced toroidal magnetic confinement devices that utilize 3-D plasma shaping to achieve steady-state operation and to optimize plasma confinement and stability. Among these, the design of compact (or low aspect-ratio) stellarators is one of the new, challenging research areas of interest in magnetic confinement. The challenge is that maintaining good transport and stability properties at low *aspect ratio* is generally more difficult than at high aspect ratio.

However, careful control of the 3-D shape appears to offer the flexibility to achieve good transport and stability characteristics. This insight has been realized through the development of sophisticated optimization codes that numerically explore 30-40 dimensional parameter spaces (the stellarator's outer flux surface shape is described in terms of 30-40 Fourier modes) and arrive at shapes that minimize a range of desired equilibrium, transport and stability physics target functions [A. S. Ware et al., "High-beta equilibria of drift-optimized compact stellarators", Phys.

Rev. Lett. **89**, 125503 (2002)]. Typical stability targets are the *Mercier criterion*, resistive interchange, high- n ballooning, and kink mode stability.

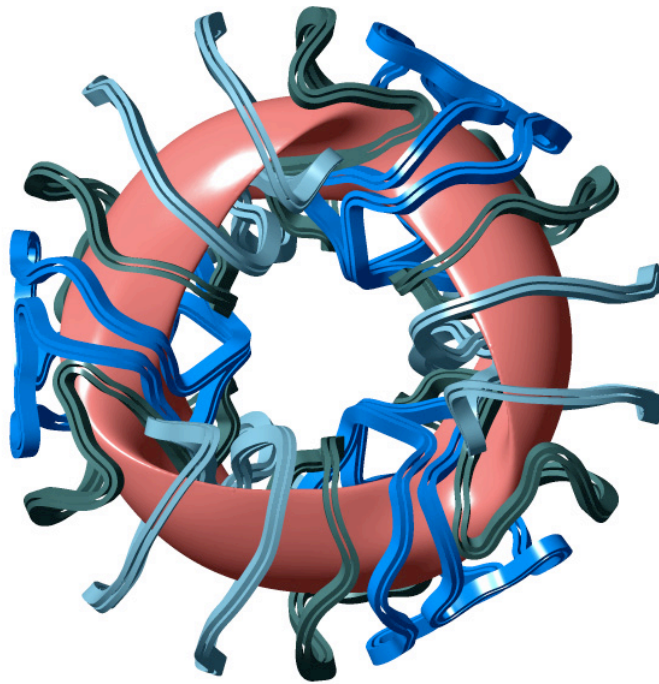


Fig. A2. *Quasi-axisymmetric National Compact Stellarator Experiment (NCSX).* [Courtesy G. H. Neilson, PPPL]

These optimization procedures have led to unexpectedly robust configurations such as the quasi-omnigenous or quasi-poloidal compact stellarator (QPS) being designed at Oak Ridge National Laboratory and the quasi-axisymmetric National Compact Stellarator eXperiment (NCSX) device [<http://www.pppl.gov/ncsx/>] currently in the design phase at Princeton Plasma Physics Laboratory. Figure A2 is a plan view of NCSX, showing the outer closed flux surface and the main magnetic coils. The integration initiative could lead to the inclusion of more sophisticated and more compute-intensive particle-transport, 3-D stability, and coil-reconstruction modules directly in the optimization. This could yield yet more surprising and robust three-dimensional configurations suitable for reactor-grade plasma confinement.

3. Turbulence Regulation by Self-Generated Flows

A major step in tokamak research was the experimental realization that the High Mode (*H-Mode*) of confinement in tokamaks was accompanied by a sudden increase in the primarily poloidal rotation of the plasma in the region of steep pressure gradient at the plasma's edge. Almost contemporaneously, early computer calculations were showing that turbulence could spontaneously generate large radial scale flows, which formed a *transport barrier* [A. Hasegawa and M. Wakatani, "Self-organization of electrostatic turbulence in a cylindrical plasma", Phys. Rev. Lett. **59**, 1581 (1987)]. This insight was later confirmed experimentally with the discovery of internal barriers, confirmed computationally with the almost universal observation of Reynolds-stress-generated flows in fluid, *gyrofluid* and *gyrokinetic* simulations, and put on sound theoretical foundations by several thorough analytical studies.

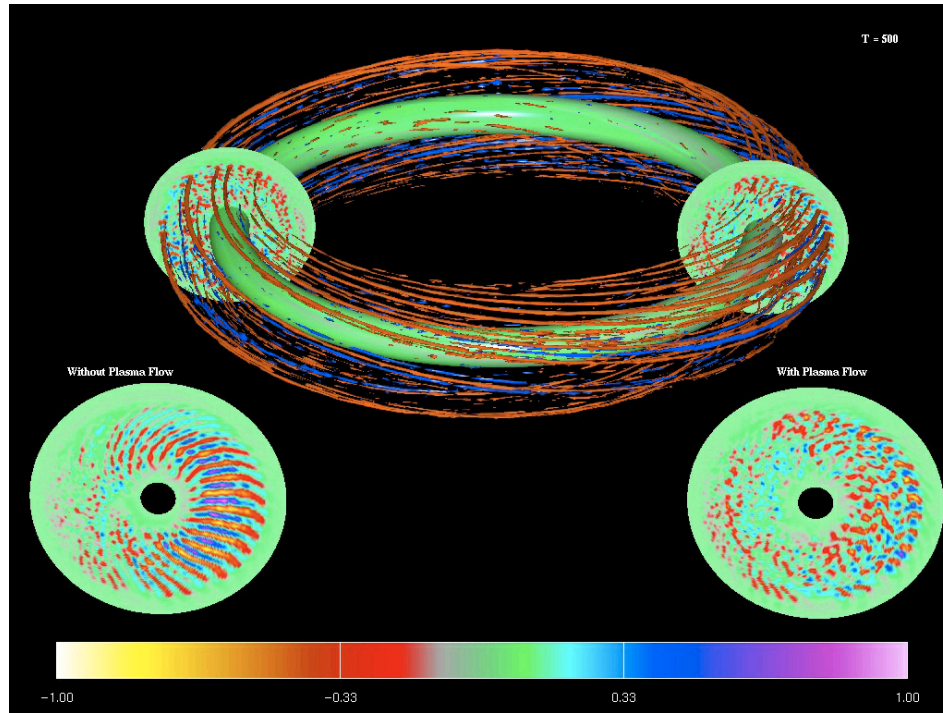


Fig. A3. *Computational evidence of flow regulation of turbulence* [Courtesy Z. Lin, PPPL/UC-Irvine]

In particular, the computations showed the effectiveness of these flows to regulate the turbulence in terms of scale size, fluctuation levels, diffusivities and therefore the transport. Recent theoretical effort motivated by differences in the characteristics of the turbulence obtained from fluid and kinetic models led to the identification of a residual flow damping mechanism, which in turn gave rise to an improvement of the computational methods. Further theoretical development has also led to the discovery of long-lived, fine radial scale flows nonlinearly generated by the turbulence or *zonal flows* whose properties and consequences were confirmed in the details by the computational models. Figure A3 represents a microturbulence simulation. Poloidal cross sections at bottom left and right show flow patterns without and with zonal flows [Z. Lin et al., “Turbulent Transport Reduction by Zonal Flows: Massively Parallel Simulations,” *Science* **281**, 1835 (1998)].

We anticipate that these kinds of insights coming from the synergy among experiment, theory, and computation, exemplified by the role of flow in regulating the turbulence, will be one of the distinguishing characteristics of the integration initiative. (See Secs. IV-VI.)

4. *Full-wave modeling of radio frequency heated, multidimensional plasmas*

A major challenge in understanding waves for fusion is that they can dramatically change character after launch, i.e. undergo *mode conversion*. At a given frequency a uniform magnetized plasma supports several different kinds of waves, with very different characters with respect to polarization, speed and wavelength, such as fast *magnetosonic* waves, slow ion-cyclotron waves and *ion Bernstein waves* (IBW). (See Sec.VII.) In a non-uniform plasma these different waves can

convert at isolated spatial locations, the classic example being conversion of the fast magnetosonic wave to an IBW at the 2-ion hybrid resonance.

Understanding this process in the realistic 2- and 3-dimensional geometries of toroidal magnetic confinement devices has required computational modeling and only recently has it become possible to fully resolve the mode conversion layer, for example with the All Order Spectrum Algorithm or AORSA code [E. F. Jaeger et al., “Advances in full-wave modeling of radio frequency heated, multidimensional plasmas”, *Phys. Plasmas* **9**, 1873 (2002)].

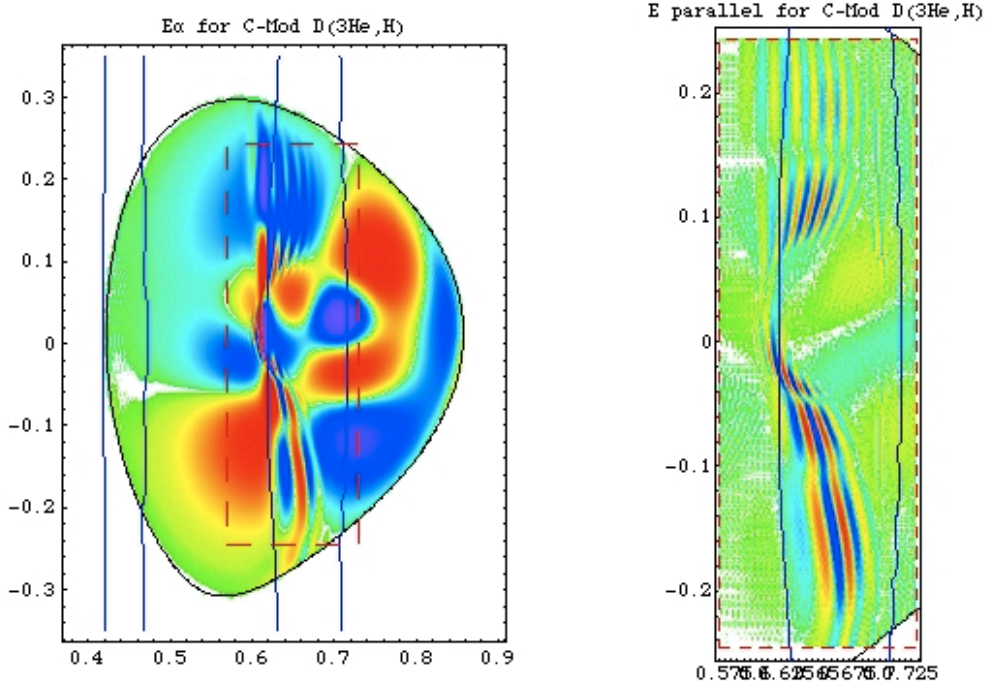


Fig. A4 Mode conversion to fast ion cyclotron wave revealed by AORSA computations. [Courtesy D. Batchelor, ORNL]

The surprise is that these realistic-geometry and well resolved calculations show that with full poloidal field the fast magnetosonic wave converts dominantly to a slow ion-cyclotron wave, not an IBW. This had been hinted at by F. Perkins who did an approximate 1-D calculation in 1977 showing that both types of conversion could, in principle, occur [F. W. Perkins, “Heating Tokamaks via the ion-cyclotron and ion-ion hybrid resonances”, *Nuclear Fusion* **17**, 1197 (1977)]. But the 1-D model did not show that one could actually get a wave in a real 2-D plasma, launched from a real antenna, to the conversion layer with the right conditions for conversion. Nor did it tell how important each process would be. The 2-D calculation gives the complete, quantitative picture, but the 1-D calculation gives the qualitative paradigm by which one understands the complete results. Figure A4 shows wave amplitudes in a cross section of the *C-Mod* tokamak, with details in the conversion layer expanded in the right-hand diagram.

As with the other examples cited, RF calculations with ever improving resolution and ever tighter coupling to more comprehensive plasma models such as those contemplated as part of this integration initiative are expected to lead to even more surprises.

B. SIMULATION CHALLENGES

1. Modeling edge physics

Overall transport and confinement are determined to a great extent by the height of the temperature *pedestal* at the plasma edge. This temperature is itself governed by phenomena that start at the wall, and propagate through the *separatrix* region and into the edge region proper. It is expected that coupled and complex models of particle and heat transport, neutral and impurity fluxes, edge-gradient induced *magnetohydrodynamic (MHD)* instabilities, and turbulence in a single computational edge framework will be required to pin down which of these mechanisms, either by itself or in combination with another, regulates the pedestal height. (See Sec. IXA.) Coupling to core plasma models will probably start with the integrated edge models providing the pedestal temperature as a boundary condition for the core before more complete integration becomes feasible through a combination of physics, algorithmic, and hardware advances.

2. Modeling turbulence on transport time scales

An integrated model of turbulence on transport time scales is a daunting physics and computational task. It is nevertheless deemed feasible at several levels, each exploiting separation of space and time scales appropriately. (See Sec. IXB.) One approach consists of iterative solutions of the macroscopic transport equations with occasional updates of the profiles and diffusivities transmitted to and from the microscopic turbulence calculations. Another entails direct coupling of transport equations to gyrofluid-type microscopic models using a physics-based, yet reduced, description of the turbulence. The result of high confidence integrated modeling of turbulence and transport might be the discovery, through computations, of new favorable operating modes, such as a new H mode, with the ultimate outcome being the determination of transport from first principles.

3. Coupling of electrons and ions in core turbulence

Integration will enable examination of the combined role of turbulence on space and time scales associated with the electrons and ions. (See Sec. IIA.) To date realistic and tractable numerical simulations of each exist separately. The expected advances in integration algorithms to bridge disparate time and space scales will enable incorporation of the dynamics of each species with realistic mass ratios, and for realistic scale sizes with respect to experiments, into one computational model that covers the full range of relevant turbulence. The benefits of these computations will be to determine the extent to which electron and ion turbulence overlap in terms of spectral range and to what extent one range of scales influences and/or regulates the transport associated with the other.

4. Extended MHD

Integration will facilitate extensions to MHD computations beyond the conventional ideal and resistive models. (See Sec. IV.) Routine incorporation of two-fluid effects will determine for instance whether *whistler wave* physics included through the *Hall term* will play as important a role in phenomena leading to plasma disruptions as it does for magnetic reconnection in space and astrophysical plasmas. Similarly, the routine inclusion of diamagnetic effects associated with

the non-scalar nature of the ion pressure tensor will reveal whether the pressure-induced plasma rotation provides a way to control MHD activity which is as effective nonlinearly as it is linearly for realistic toroidal plasmas. Moreover, the inclusion of minority ion species with non-Maxwellian populations either as gyrofluids or full-fledged particle species will enable extended MHD models to describe the essential macroscopic physics of burning plasmas. Such features will provide new intuition regarding the effect of energetic particles on large-scale MHD instabilities and vice-versa.

5. The burning plasma experiment

Perhaps the greatest advances afforded by integrated modeling will be realized for burning plasmas. The grand challenge in the world fusion program is the burning plasma experiment, a necessary predecessor to a practical power reactor because, by its very nature, it presents a new category of technical issues. All other fusion experiments obtain the required plasma temperatures by applying energy sources from outside the plasma. A burning plasma – a self-sustaining energy source – maintains them through the action of the ongoing fusion reactions, which produce energetic alpha particles and high-energy neutrons. The charged alphas are trapped by the magnetic field and transfer their kinetic energy to the plasma, thus maintaining the temperatures necessary for fusion to continue.

With self-heating as the dominant plasma heating mechanism, new plasma processes and effects will arise. The high flux of energetic particles will impact the plasma wave structure, alter the plasma pressure and current profiles, and produce, through alpha-particle and neutron collisions, a rich source of wall interaction phenomena. Most seriously, all these effects will be strongly coupled and must be understood and managed in an integrated fashion to insure the stability and success of the experiment. The fully integrated fusion simulator will be targeted to model these processes and their consequences, thereby providing the essential insights to guide experimental programs, optimize machine design, and deepen our understanding of the fundamental science.

II. FUSION SCIENCE BASIC CONCEPTS

The fundamental problem in fusion science is to understand and control the physical processes that determine the balance between heating and fueling, on the one hand, and loss of confinement, on the other. The losses can come from macroscopic processes leading to breakup of the nested magnetic flux surfaces and disruptions or from microscopic processes, leading to transport across the flux surfaces. Figure 5A shows a tokamak cross-section, schematically illustrating some of the processes that will be discussed in the following sections. A cutaway view of this device is shown in Fig. III.1 of the main report.

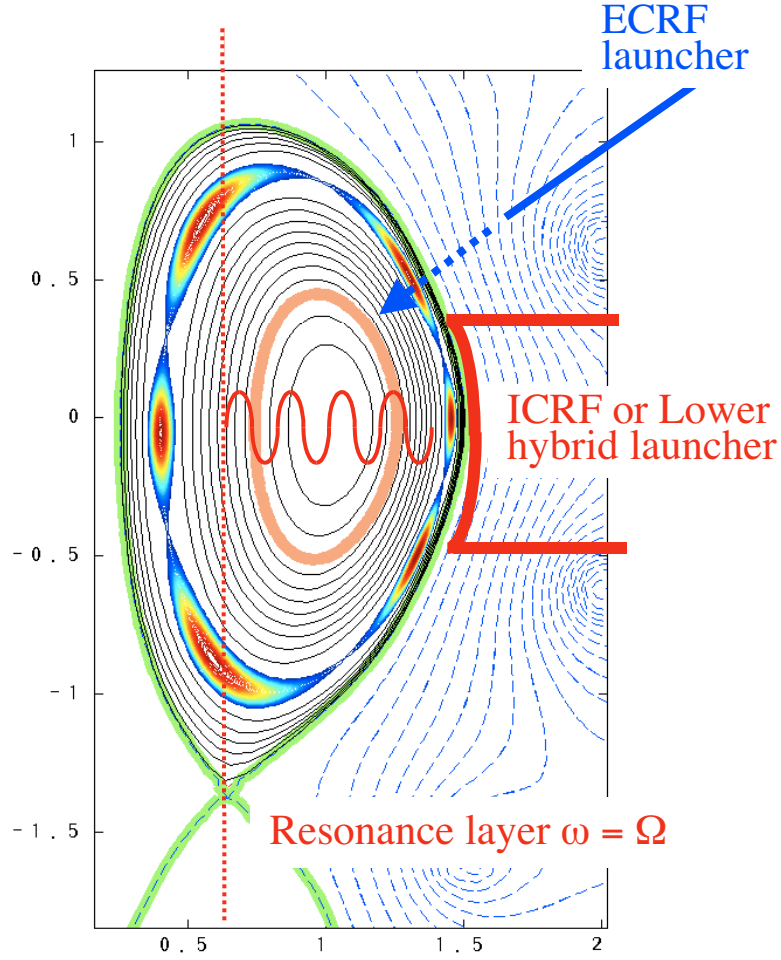


Fig. A5. Tokamak cross-section with launchers, a schematic wave and resonance layer. Here $\Omega = \omega_c$. Also shown is a chain of magnetic islands.

We begin in Part A by introducing the basic equations and concepts of plasma physics, which are the foundation of the subsequent sections, and which give rise to the time-scale chart appearing as Fig. III.2 of the main report. Reproducing this chart in Part B, we briefly outline these time scales.

A. BASIC EQUATIONS

The time-dependent processes governing the stability and confinement of the plasma are governed by the Maxwell-Boltzmann system of equations, which we write in MKS units. We begin with the distribution function $f_a(\mathbf{x}, \mathbf{v}, t)$, which is the density of charged particles of species a in a six-dimensional phase space. This function evolves in time, t , according to the Boltzmann equation,

$$\frac{\partial f_a}{\partial t} + \mathbf{v} \cdot \nabla f_a + \frac{q_a}{m_a} [\mathbf{E} + \mathbf{v} \times \mathbf{B}] \cdot \nabla_{\mathbf{v}} f_a = C(f_a). \quad (\text{A-1})$$

The characteristics of the left-hand side are the particle orbits, the second term, $\mathbf{v} \cdot \nabla f_a$, being the convection in space and the third term, $(q_a/m_a)(\mathbf{E} + \mathbf{v} \times \mathbf{B}) \cdot \nabla_{\mathbf{v}} f_a$, being the acceleration in velocity space arising from the *Lorentz force*, where \mathbf{E} and \mathbf{B} are the electric and magnetic fields, and q_a and m_a are the charge and mass of species a . Solution of the equation can begin with integration along the characteristics. (A brief Introduction to these is given in Sec. XI.) This is complicated, however, both by the right-hand side of the equation, which represents all sources, sinks, and collisional dissipation, and by the nonlinearity of the whole system. That is, the fields themselves include not only the externally generated \mathbf{B} , but also spontaneous perturbations and injected waves that depend on the particle distributions through the Maxwell equations,

$$\nabla \times \mathbf{B} = \mu_0 \mathbf{J} + \mu_0 \epsilon_0 \frac{\partial \mathbf{E}}{\partial t}, \quad \nabla \cdot \mathbf{B} = 0, \quad (\text{A-2})$$

$$\nabla \times \mathbf{E} = -\frac{\partial \mathbf{B}}{\partial t}, \quad \nabla \cdot \mathbf{E} = \rho/\epsilon_0, \quad (\text{A-3})$$

where \mathbf{J} and ρ are the sums of individual species current and charge densities,

$$\mathbf{J}(\mathbf{x}, t) = \sum_a \mathbf{J}_a(\mathbf{x}, t) = \sum_a q_a \int d^3 \mathbf{v} \mathbf{v} f_a(\mathbf{x}, \mathbf{v}, t), \quad (\text{A-4})$$

$$\rho(\mathbf{x}, t) = \sum_a \rho_a(\mathbf{x}, t) = \sum_a q_a \int d^3 \mathbf{v} f_a(\mathbf{x}, \mathbf{v}, t). \quad (\text{A-5})$$

Theoretical and computational challenges. Equations (A-1)-(A-3) generate an enormous array of phenomena. We shall touch upon the more important of these in the following sections. The sources of this complexity are:

1. The complex structure of the confining magnetic fields, which give rise to multiple classes of orbits even in the absence of perturbations,
2. The long-range nature of the electromagnetic forces, which give rise to collective phenomena, both externally driven and spontaneously occurring waves and instabilities.
3. The great range of space and time scales and extreme anisotropy of both individual particle motions and plasma waves, extending from the size of the device (a few meters) and the duration of the discharge (exceeding several minutes in a recent record-setting experiment) all the way down to the electron *gyroradius* and *gyrofrequency*, and
4. Dissipation, i.e., collisions among ion species and electrons, as well as those with neutrals (sources and sinks), all buried in the term $C(f_a)$ on the right-hand side of Eq. (A-5). Even when the collision term itself is negligibly small, dissipation occurs and plays a major role, owing to *wave-particle resonances*, and nonlinear decorrelation of waves.

An electron in a uniform magnetic field \mathbf{B} orbits the field line in a perpendicular plane (Part B, below) with gyrofrequency $\omega_{ce} = eB/m_e \approx 5 \times 10^{11} \text{ s}^{-1}$ and with gyroradius $\rho_{ce} = v/\omega_{ce} \approx 6 \times 10^{-5} \text{ m}$. (These numerical values are for a typical plasma temperature of 3 keV and a typical magnetic field strength of $B = 3 \text{ T}$.) Frequencies and wavelengths for the highest range of radio-frequency wave heating are of the same order. (Ions gyrate with frequency lower and radius larger by m_e/m_i and $\sqrt{m_i/m_e}$, respectively.) The same electron moves freely parallel to the field, but in the curved and spatially varying fields of a torus, it is subject to additional slower drifts and accelerations on the whole device scale, of order $2\pi R \approx 10 \text{ m}$ in present-day machines, where R is the *major radius*.

Thus, our phenomena extend over a range of 9-10 orders of magnitude in time and, perpendicular to the magnetic field, 4-5 orders in space. For much of our work, we can also average over the gyro-motion, reducing our equation to five phase-space dimensions (*gyrokinetic theory*), and increasing the time step by another order of magnitude. Even so, one estimate of the coverage needed for a full-discharge simulation would require 10^{11} phase-space points at 10^8 time steps. Not only does this far exceed our present capability, but also we would not be able to store or analyze the output from such a calculation.

Actual plasma computations, therefore, are carried out by means of ordering schemes leading to approximations that focus on particular scales and are valid for particular phenomena. Beginning with Eqs. (A-1)-(A-3), the equations to be solved are obtained by averaging over the finer space and time scales and applying some prescription for closure. For example, in a toroidal device, particles drift away from magnetic surfaces at a rate slower than the gyration by factors of order $\rho^* = \rho_{ci}/a$, where a is the minor radius. Relatively infrequent collisions or decorrelations then allow transport losses described by a random walk with diffusivity of the form $D \sim (\delta x)^2/\delta t$ where δx and δt , the characteristic step size and collision time, exceed the shortest scales given above. *If D and related quantities can be simply characterized*, then the resulting transport equations are solved on still longer time and space scales. Whole-device simulation currently proceeds in this manner, but the “if” in the preceding sentence is a big one.

Much progress has been made in the major subfields of plasma theory and computation, which we describe in the following sections. Figure III.2 in the main report, repeated as Fig. A6 in the next section, shows a chart of the principal frequency ranges and the phenomena associated with them.

The great challenge and opportunity before us is to further develop and combine these in a tractable way, leading to whole-device simulation that contains complete and reliable models of all the relevant physics.

B. REDUCED DESCRIPTIONS

The codes currently in use are each based on different approximations to the full set of plasma equations (A-1) to (A-3) that isolate phenomena in a more restricted range of frequencies. Together, they span the ranges of frequency described above. A summary of the four major code groups presently in use and the timescales being addressed by them is given in Fig. A6.

Typical Time Scales in a next step experiment with $B = 10 \text{ T}$, $R = 2 \text{ m}$, $n_e = 10^{14} \text{ cm}^{-3}$, $T = 10 \text{ keV}$

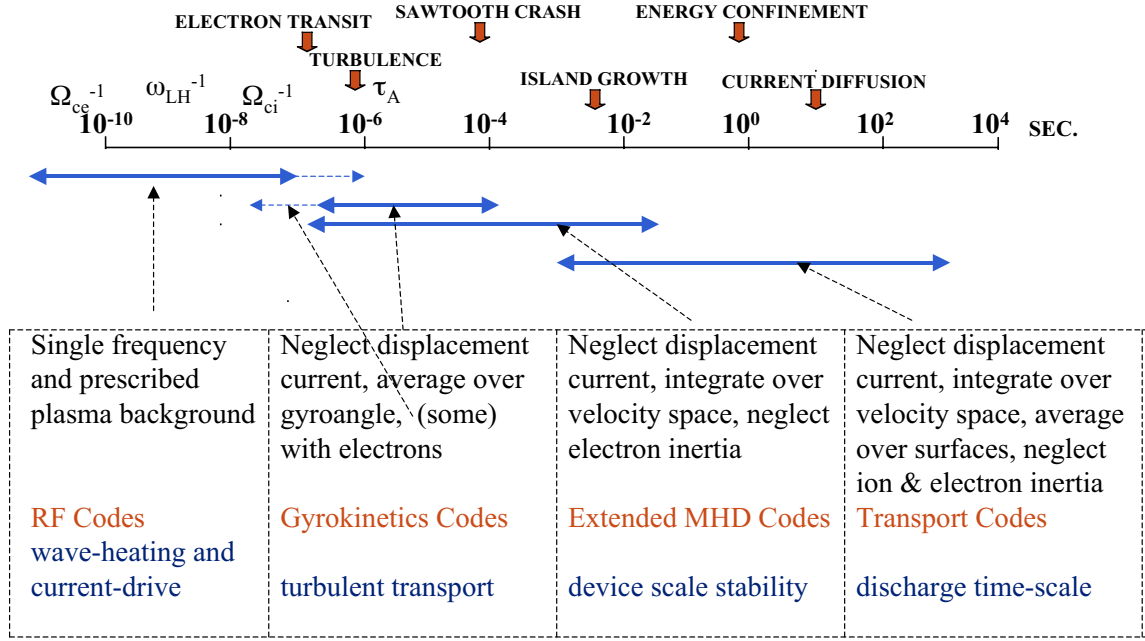


Fig A6. Summary of the four major code groups and the timescales being addressed.

The RF codes (external sources) address frequencies of order the ion cyclotron frequency, Ω_{ci} , and above, up to the electron cyclotron frequency Ω_{ce} . (This notation is used interchangeably with ω_{ci} and ω_{ce} .) They assume a single, fixed frequency set by the oscillator, and solve for the linear and quasi-linear response of a given background plasma to the imposed electromagnetic fields at this frequency. They are used to calculate wave-heating and current-drive by radio-frequency (RF) sources.

The gyrokinetics codes (microscopic modeling) are based on an analytic averaging of the full kinetic equation to eliminate the fast gyro-orbit frequencies from the equations. They and the other codes described below also neglect the displacement current term in Maxwell equation (A-2) to remove light waves from the system. These reductions allow them typically to take time steps about 10 times longer than the ion cyclotron frequency (whose motion is analytically averaged over) and are normally run for 10^3 to 10^4 time steps to calculate stationary turbulent fluctuation levels. Recent additions to these codes to include some electron timescale phenomena bring in the electron transit time, which lowers the maximum time step.

The Extended MHD codes (macroscopic modeling) are based on taking velocity moments (or weighted integrals over velocity space) of Eq. (A-1) to obtain fluid-like equations that describe large-scale phenomena more efficiently. They aim to resolve phenomena occurring on the Alfvén

transit time, τ_A , although most codes are at least partially implicit to avoid a strict restriction on the time step based on this. These codes can normally run 10^4 to 10^5 time steps to address MHD phenomena such as sawteeth and island growth.

The 2-D transport codes (equilibrium evolution and confinement) further simplify the equations by eliminating the Alfvén waves and by averaging plasma properties over 2-D magnetic surfaces. These codes are very efficient and can take many long time steps to model the entire discharge. However, the 2-D edge transport codes need to resolve the parallel dynamics and use a time-step based on the parallel sound-wave propagation near the edge region.

The following sections describe each of these code groups in more detail.

III. MICROSCOPIC SIMULATION

A. INTRODUCTION AND SUMMARY

This section deals with the direct calculation of the microscopic processes that affect the quality of a magnetic field configuration as a thermal insulator. Loss of plasma particles and energy across field lines results from at least three categories of microscopic phenomena: diffusion and convection based on individual orbits and collisions (classical, neoclassical), anomalous diffusion and convection from turbulent microinstabilities (usually thought to be dominant), and phenomena that are instantaneous and non-local.

- Neoclassical codes for both 2- and 3-D configurations are available subject to certain approximations. Additional work will be required to implement fully the existing theories and to account for additional effects in the inter-operative environment.
- Micro-turbulence-driven anomalous transport will be dealt with on three levels: a) fine-scale stand-alone gyrokinetic simulations of core plasma turbulence will continue to be developed, interpreted by theory, and compared with experiment to firmly validate the fundamental theory and benchmark the other descriptions; b) reduced simulations will be coupled directly to the transport equation solvers. In some cases, it may be possible to couple directly the full turbulence simulations with the transport equation solvers (a topic of one of our focused initiatives); and c) algebraic models of transport will continue to be developed, again informed by theory, experiment, and the just-described simulations. When supported by turbulence simulations for selected cases, they will provide the most rapid parameter scans
- Work will continue on development of models of observed rapid and non-local phenomena (e.g. avalanches, radiative transport, or global magnetic interactions) that do not fit into the diffusive-convective approach. The architecture must include provision for these from the outset, so they can be incorporated when available.

A measure of success for these efforts and their validation will be the ability to predict and model a transport barrier, a region of steep gradients where turbulence is suppressed. This will involve integrated treatment of the radial electric field as also mentioned in Secs. V and VI.

B. NEOCLASSICAL TRANSPORT

At the most basic level, transport is a random-walk process, in which a particle drifts slowly away from a magnetic flux surface and from time to time suffers a collision that transfers it to a new orbit. The resulting diffusivities have the form $D, \chi \sim (\delta x)^2 / \delta t$ where δx and δt are the characteristic step size and collision time. The detailed task of *neo-classical theory* is to compute the flux-surface averaged fluxes (see Sec. VI, Eqs. (A-24)-(A-25)) by solving a gyro-averaged form of the Boltzmann equation (A-1), called the *drift-kinetic equation*. Closure is provided in an ordering in which the collision operator is dominant, and the step size (drift orbit) is small compared to the plasma gradient scale length. (*Classical transport*, in which the step size is of the order of the gyroradius ($\delta x \sim \rho_a$), is small and most often neglected in fusion calculations.)

Neoclassical theory is highly developed in the limit that finite orbit-width effects (violation of the above ordering) and energy scattering are unimportant. Codes for both 2- and 3-D configurations are available subject to these approximations. Additional theoretical work and extensive code development will be necessary in order to account for a number of important phenomena associated with neoclassical theory such as: neoclassical transport when barriers turn off the anomalous transport, *bootstrap* effects (neoclassical currents driven by gradients), non-local orbit effects such as *potato orbits* (orbits near the plasma center), self-consistent electric field effects in non-axisymmetric configurations, impurity transport etc. Additional work will be required to fully implement the existing theories in the “interoperative” environment, particularly in 3-D configurations (stellarators) and in tokamaks with transport barriers. To treat the mutual interaction of islands or stochastic magnetic fields with neoclassical driven transport and currents will require extensive further development.

C. TURBULENCE AND ANOMALOUS TRANSPORT

Gradients of plasma density and temperature provide the free energy to drive micro-instabilities that lead to anomalous transport. These waves typically propagate with phase velocities perpendicular to the field of order $v_a^* = \rho_a v_a d \ln n_e / dr$ (see Sec. XI, Eq. (A-30)), or $v_{Ta}^* \ll v_a$ where the temperature gradient replaces the density gradient. This gives rise to the characteristic *diamagnetic frequencies* $\omega_a^* = k_\perp v_a^*$ and $\omega_{Ta}^* = k_\perp v_{Ta}^*$ in a wave $\tilde{\phi} \sim \exp(i\mathbf{k}_\perp \cdot \mathbf{x})$, where $k_\perp \sim \rho_a^{-1}$, for $a = i$ (ion waves) or $a = e$ (electron waves). The waves are known generically as *drift waves*, particular examples of which are the *ion temperature-gradient* (ITG) modes and *electron temperature-gradient* (ETG) modes.

To evaluate these we begin with the Maxwell-Boltzmann system, Eqs. (A-1)-(A-5), neglecting displacement current and charge density (*quasi-neutrality*). Averaging over the gyro-angle, we obtain the *guiding center* distribution $F_a(\mathbf{x}, \mathbf{v}, t) = F_{0a}(\rho, W) (1 + q_a \tilde{\phi} / T_a) + \tilde{h}_a(\mathbf{x}, W, \mu, t)$ in a 5-dimensional phase space, where the velocity variables are the magnetic moment $\mu = mv_\perp^2 / 2B$ and kinetic energy $W = mv^2 / 2 = \mu B + mv_\parallel^2 / 2$. It is convenient to separate out the background distribution $F_{0a}(\rho, W)$ and the so-called *adiabatic part* $F_{0a}(\rho, W) q_a \tilde{\phi} / T_a$. (The latter is actually the lowest order solution in one important limit.) The remaining part of the distribution, \tilde{h}_a

obeys the *gyrokinetic equation*, in which the convective term in (A-1) is replaced by a similar term with gyro-averaged particle drifts replacing the velocity \mathbf{v} :

$$\frac{\partial \tilde{h}_a}{\partial t} + (\mathbf{v}_{\chi a} + \mathbf{v}_{da} + v_{\parallel} \hat{\mathbf{b}}) \cdot \nabla \tilde{h}_a = -\mathbf{v}_{\chi a} \cdot \nabla f_{0a} - q_a \frac{\partial f_{0a}}{\partial W} \frac{\partial \tilde{\chi}}{\partial t} \quad (\text{A-6})$$

+ collisions + sources/sinks,

where $\hat{\mathbf{b}}$ points in the direction of the equilibrium magnetic field, \mathbf{v}_{da} is the curvature- and grad-B drift, and the $\mathbf{E} \times \mathbf{B}$ drift is combined with transport along perturbed magnetic fields lines and the perturbed grad B drift as

$$\mathbf{v}_{\chi a} = \hat{\mathbf{b}} \times \nabla \chi_a / B, \quad (\text{A-7})$$

where

$$\chi_a = \left(\left\langle \tilde{\phi} - v_{\parallel} \tilde{A}_{\parallel} \right\rangle_g + \left\langle \mu \tilde{B}_{\parallel} / q_a \right\rangle_g \right) / B. \quad (\text{A-8})$$

Here, we represent the fluctuating fields in terms of the potentials $(\tilde{\phi}, \tilde{A}_{\parallel})$ plus \tilde{B}_{\parallel} and denote the gyro-average by the angle brackets $\langle \dots \rangle_g$. The principal nonlinearity of Eq. (A-6) is the perturbed convective term $\mathbf{v}_{\chi a} \cdot \nabla \tilde{h}_a$.

To illustrate the method and make contact with theory, we note that the gyrokinetic ordering requires a separation of scales that lends itself to an eikonal representation, i.e., a perpendicular expansion of fluctuations as $\exp(iS)$ where $\nabla S = \mathbf{k}_{\perp}$ may be interpreted as the perpendicular wave vector. In this case, Eq. (A-8) may be evaluated as

$$\tilde{\chi}_a = J_0(b_a) (\tilde{\phi} - v_{\parallel} \tilde{A}_{\parallel}) + J_1(b_a) / b_a (\mu \tilde{B}_{\parallel} / q_a). \quad (\text{A-9})$$

The Bessel functions J_0 and J_1 have argument $b_a = k_{\perp} v_{\perp} / \omega_{ca}$. Of course, in a non-uniform medium the perpendicular wave number is really a differential operator. (In order to evaluate these functions efficiently, the codes we will describe make extensive use of numerical Fourier transformation and its inverse.) In particular, the gyro-averaged wave potential is given by

$$\langle \tilde{\phi} \rangle_a(\mathbf{x}) = \frac{1}{2\pi} \oint d\zeta \tilde{\phi}(\mathbf{x} + \rho_a) = J_0(k_{\perp} \rho_a) \tilde{\phi}(\mathbf{x}), \quad (\text{A-10})$$

where ζ is the gyro-angle, as illustrated in Fig. A7.

Finally, the Maxwell equations are recast in potential form, e.g.,

$$\nabla^2 A_{\parallel} = -\mu_0 \sum_a q_a \int d^3 v v_{\parallel} J_0(b_a) \tilde{h}(a), \quad (\text{A-11})$$

where the right-hand side is the parallel current.

We draw attention to the fact that solving the *continuum* Eq. (A-6) is equivalent to following gyro-averaged orbits of an ensemble of discrete particles,

$$F_a = \sum_{i=1,N} w_i(t) \delta(\mathbf{x} - \mathbf{x}_i(t)) \delta(\mathbf{v} - \mathbf{v}_i(t)), \quad (\text{A-12})$$

with suitable particle smoothing, Monte Carlo treatment of collisions, sources and sinks.

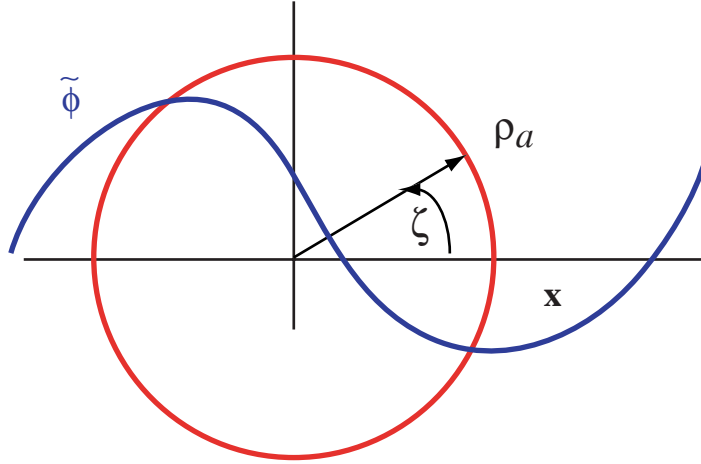


Fig. A7 Gyro-orbit average of perturbed potential.

The system consisting of Eq. (A-6) and the Maxwell equations, Eqs. (A-2)-(A-3) (neglecting the displacement current,) drives turbulence on scales ranging from the electron to the ion gyroradius, as noted at the beginning of this section. The linear and nonlinear growth and damping mechanisms have been well delineated theoretically, and a number of codes are able to compute the evolution and saturation of the waves *and the resulting flux-surface-averaged transport fluxes* (see Sec. VI). The codes are of four types. Each may be either *flux-tube* (localized perpendicular to the field) or *global* (covering a major fraction of the plasma radius). Also, each may be either *continuum* (solving Eq. (A-6) on a fixed Eulerian grid), or *particle-in-cell* (or PIC, following an ensemble of gyro-averaged particles in a Lagrangian formulation) as in Eq. (A-12). All four types of code have advantages and disadvantages.

The SciDAC numerical turbulence project supports a two-by-two matrix of codes:

	Continuum	PIC
Flux tube	GS2	SUMMIT
Global	GYRO	GTC

There are both continuum and PIC because continuum is currently the most developed (kinetic electrons, important even for waves on the ion gyro-scale, and perturbed magnetic fields) while PIC may be ultimately more efficient. A flux tube is described in coordinates that are extended along field lines but are localized in perpendicular directions. There are high-resolution *flux-tube codes* to support multiple space and time scales (electron and ion gyro-physics) and validation of

local turbulence physics (rapid parameter scans). *Global codes*, which provide calculations over a major fraction of the plasma radius, are needed to account for extended profile effects and are most likely the best bet for coupling to the integrated simulation.

The plasma turbulence is quasi-2-dimensional because of the plasma anisotropy. The current state-of-the art in global PIC simulations with GTC, without including full electron dynamics or magnetic perturbations, is the following. The resolution requirement along \mathbf{B} is determined by the equilibrium structure. The structure across the field is determined by the microstructure of the turbulence, $\sim \rho_{ci}$ for *ion temperature-gradient (ITG) modes*. This requires $\sim 64 \times (a/\rho_{ci})^2 \sim 2 \times 10^8$ grid points and 8 particles per spatial grid point, where a is the minor radius of the machine. This leads to $\sim 1.6 \times 10^9$ particles and 1 terabyte of RAM for 600 bytes/particle. This resolution is currently achievable. The time scale is on the order of $a/v_i \sim 1 \mu\text{sec}$ for 10 time steps. To simulate many correlation times corresponding to a simulation of a few ms requires about 90 hours of IBM SP (SEABORG) time at 4×10^9 sec/particle-timestep. This is heroic, but the discharge time actually simulated is much smaller than the plasma equilibration time.

The situation is similar for continuum codes. GYRO, in particular, has the most complete physics to date for ion gyro-scale physics: ions and electrons (trapped and passing), magnetic perturbations and collisions, real geometry, nearly full radius, finite $\rho^* = \rho_{ci}/a$ with profile and $\mathbf{E} \times \mathbf{B}$ shear stabilization and toroidal velocity-shear drive. Simulation of a single radial slice ($\Delta r/a = 0.3$) of DIII-D plasma for about 1ms takes five 24-hour submissions on 128 processors on SEABORG. Scaling from DIII-D to ITER and taking full radius requires a factor of 15. The 1ms rescales to 2ms but it is still a long way from 3 sec confinement times. This reflects the fact that going beyond the previous state of the art from ions-only simulations to simulations with electron dynamics requires an order of magnitude jump in computing power because the required time step is at least 10 times smaller. Output from GYRO is shown in Fig. A8, showing the strong anisotropy.

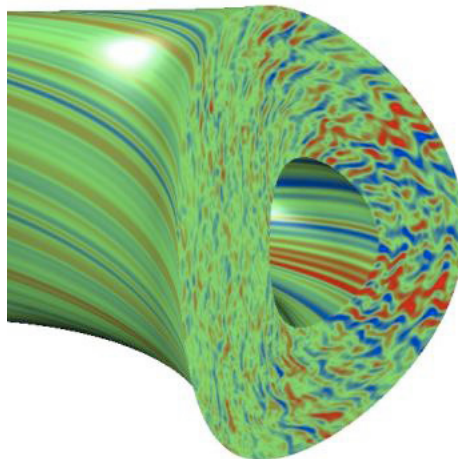


Fig. A8. *Ion temperature-gradient turbulence in GYRO simulation. Extended structures along the field lines are evident. [Courtesy J. Candy, GA]*

D. NON-LOCAL PHENOMENA

We cannot leave this discussion without taking note of observed phenomena in tokamaks that seem to defy the diffusion-convection picture. These include extremely rapid (i.e. faster than the transport time scale) propagation of heat pulses (or “cold” pulses) resulting from sawtooth crashes, impurity injection at the edge, or the H-mode transition itself. There are two current approaches to explain these observations. First, there are empirical techniques based on the concepts of *self-organized criticality* (SOC) and *avalanches*. Empirical models have given good results, but the underlying physics has not been elucidated. Second, the instabilities leading to turbulence usually have fairly well defined thresholds, e.g., a critical temperature gradient. A rapid pulse may occur if the plasma is perturbed from its marginal condition. In this case, the underlying physics is presumed known, but quantitative calculations have not been performed. The simulation project must be prepared to incorporate developments in this area.

E. CHALLENGES FOR TURBULENCE SIMULATIONS

The bottom line is that we are currently far from the achievement of turbulence simulations with all the relevant physics on a scale suitable for integration with transport calculations. One estimate, presented at the May 23 ISOFS Workshop, is that we are six orders of magnitude from a solution based on current computational methods and computers, and that we will make up only four of these orders in the next few years by advances in computer technology and currently envisioned schemes for exploiting the time-scale separation (see Sec. IXB). Among the computational and applied mathematical challenges are:

- Continuum kernels solve an advection/diffusion equation on a 5-D grid; we therefore need: linear algebra and sparse matrix solvers (LAPAC, UMFPAC, BLAS), and distributed array redistribution algorithms.
- Particle-in-Cell kernels advance particles in a 5-D phase space and need: efficient “gather/scatter” algorithms that avoid cache conflicts and provide random access to field quantities on a 3-D grid.
- Continuum and Particle-in-Cell kernels perform elliptic solves on 3-D grids (often mixing Fourier techniques with direct numerical solves).
- Other Issues are portability between computational platforms, characterizing and improving computational efficiency, distributed code development, and expanding the user base.

Finally, we note that while core turbulent transport is extremely important (ability to predict internal barriers, for example), edge turbulence, which has the same difficulties described here and more (Sec. VIII), is critical, for the edge pedestal is the greatest source of uncertainty for reactor predictions.

IV. MACROSCOPIC SIMULATION

A. INTRODUCTION AND SUMMARY

Coupled magnetohydrodynamics (MHD) and Maxwell equations play a central role in modern fusion plasma theory. First, MHD determines 2-D or 3-D magnetic equilibrium with nested toroidal magnetic flux surfaces, which are crucial for magnetic plasma confinement. Next, MHD describes both thresholds and nonlinear dynamics of device-scale plasma instabilities (so called MHD instabilities). Very often these instabilities set the limits of the performance of fusion devices.

Plasma dynamics can be completely described by the evolution of the distribution function $f_\alpha(\mathbf{r}, \mathbf{v}, t)$, for each particle species α , given by each species plasma kinetic equation, together with the self-consistent evolution of the electric and magnetic fields, given by the Maxwell equations, as given in Eqs. (A-1)-(A-6). Solving these equations for space scales and timescales characteristic of large-scale instabilities in confined plasmas is computationally impractical. The Extended MHD approach is to reduce the dimensionality of the problem, by multiplying the kinetic equation by successive powers of the particle velocity \mathbf{v} and integrating over velocity space. If the underlying distribution functions have nice properties, such as a close-to-Maxwellian velocity distribution, the resulting moment equations have fluid-like properties. They are more tractable theoretically and computationally, although formidable problems may still arise.

Magnetic fusion devices are very rich in MHD activity, some relatively benign, some leading to catastrophic disruptions. Some of these are known as *sawtooth oscillations*, *tearing* and *ballooning instabilities*, and *resistive wall modes*, whose general features and some quantitative predictions can be given in terms of ideal or resistive MHD. As higher plasma temperatures are reached, more and more kinetic effects are required to be included.

B. EQUATIONS

On the time and space scales that the electrons and ions maintain local charge neutrality, the lowest order moment equations for the electron and ion species can be added together to form a set of equations for a plasma fluid with a density $\rho = (M_i n_i + m_e n_e)$, fluid velocity $\mathbf{v} = (M_i n_i \mathbf{v}_i + m_e n_e \mathbf{v}_e) / (M_i n_i + m_e n_e) \sim \mathbf{v}_i$ and pressure $p = p_i + p_e$. (Note that the symbol ρ is being used here for the mass density. The same symbol has elsewhere been used to represent charge density and normalized minor radius.) The displacement current can be neglected in Ampere's law (since $\nabla \cdot \mathbf{J} = 0$), eliminating electromagnetic radiation and electrostatic oscillations. The MHD equations can be written in a general form, in MKS units, as the low-frequency Maxwell equations,

$$\frac{\partial \mathbf{B}}{\partial t} = -\nabla \times \mathbf{E} \quad , \quad \nabla \times \mathbf{B} = \mu_0 \mathbf{J} \quad , \quad \nabla \cdot \mathbf{B} = 0 \quad , \quad (\text{A-13})$$

the continuity equation,

$$\frac{\partial \rho}{\partial t} = -\nabla \cdot \rho \mathbf{v} \quad , \quad (\text{A-14})$$

the total momentum equation,

$$\rho \left(\frac{\partial \mathbf{v}}{\partial t} + \mathbf{v} \cdot \nabla \mathbf{v} \right) = -\nabla \cdot \mathbf{P} + \mathbf{J} \times \mathbf{B} \quad , \quad (\text{A-15})$$

and the energy equation,

$$\frac{\partial p}{\partial t} + \mathbf{v} \cdot \nabla p = -\frac{5}{3} p \nabla \cdot \mathbf{v} - \frac{2}{3} (\mathbf{\Pi} : \nabla \mathbf{v} - \nabla \cdot \mathbf{q} + Q). \quad (\text{A-16})$$

The energy equation (A-16) assumes that the ratio of specific heats $\gamma = \gamma_e = \gamma_i = 5/3$. In these equations, μ_0 is the permeability of free space, n is the number density, ρ is the mass density, \mathbf{v} is the center of mass velocity, \mathbf{B} is the magnetic flux density, \mathbf{E} is the electric field, \mathbf{J} is the current density, p is the scalar pressure, \mathbf{q} is the heat flux, η is the electrical resistivity, the stress tensor is $\mathbf{P} = p\mathbf{I} + \mathbf{\Pi}$, where \mathbf{I} is the unit tensor and $\mathbf{\Pi}$ is the traceless part of the stress tensor, and Q is other heat sources and sinks.

In general, the electron motion decouples from the bulk fluid motion, although the two are related by $\mathbf{v} = \mathbf{v}_e + \mathbf{J}/ne$. For near-Maxwellian distribution functions, for example, decoupling can occur due to the effects of a non-negligible ion *Larmor radius* (*finite Larmor radius* or *FLR*), which is still small relative to the system size. The equation for the electric field, known as Ohm's law, comes from the electron momentum equation. Ignoring terms of order m_e/M_p , it is

$$\mathbf{E} = -\mathbf{v} \times \mathbf{B} + \eta \mathbf{J} + \frac{1}{ne} \mathbf{J} \times \mathbf{B} - \frac{1}{ne} \nabla \cdot \mathbf{P}_e - \frac{1}{ne} \rho_e \left[\frac{\partial \mathbf{v}_e}{\partial t} + \mathbf{v}_e \cdot \nabla \mathbf{v}_e \right] \quad (\text{A-17})$$

It requires a pressure or temperature equation for the electrons,

$$\frac{\partial p_e}{\partial t} + \mathbf{v}_e \cdot \nabla p_e = -\frac{5}{3} p_e \nabla \cdot \mathbf{v}_e - \frac{2}{3} (\mathbf{\Pi}_e : \nabla \mathbf{v}_e - \nabla \cdot \mathbf{q}_e + Q_e) \quad , \quad (\text{A-18})$$

Additional detail, still within the confines of a two-fluid moment description, can be obtained by keeping the anisotropies relative to the confining magnetic field, such as the two pressures p_\perp and p_\parallel and/or the heat fluxes. The above equations then refer to the average quantities $p_j = (p_{j\parallel} + 2p_{j\perp})/3$, etc.

To close the system, expressions for the higher order moments $\mathbf{\Pi}$ and \mathbf{q} must be obtained independently, from solutions to the kinetic equation. At high collisionality, these are the usual collisional viscous stress tensor and the heat flux (proportional to the local velocity and temperature gradients, respectively), and this leads to the *Braginskii equations*. At lower

collisionality or long mean free path, these terms contain non-local kinetic effects. Proper closure becomes a complex question that must take into account details of the confinement configuration. (In toroidal systems, these non-local geometrical effects have been addressed in a flux-surface-averaged sense by neoclassical theory.) Unfortunately also, in this limit there is no single, unambiguous way to define the set of “two-fluid” or FLR terms, so that models depend upon a mixture of theoretical and practical considerations (see R. D. Hazeltine and J. D. Meiss, *Plasma confinement*, Addison Wesley, 1992.)

Another approach that is being pursued is the so-called hybrid approach where a distribution of particles is used to provide closure to the fluid equations. There are 2 categories of the hybrid approach that are being used: pressure coupling and current coupling. Even within these categories, there are several approaches.

In the *pressure-coupling scheme*, the distribution of particles is used to calculate the pressure tensor, and then the velocity is advanced in time from Eq. (A-15). The pressure tensor has been calculated differently by different researchers: from the gyroviscous stress tensor in terms of gyrofluid moments; by using approximations to the gyroviscous stress tensor given in terms of Bessel functions in Fourier-Ballooning space; by using a particle Hall-MHD closure that uses test particles to compute the off-diagonal elements of the pressure tensor; or by calculating the stress tensor directly from summing moments of Gyrokinetic particles.

In the *current coupling scheme*, the ion current is calculated directly from the particles, and no fluid ion equations of motion is needed. This has been implemented using the full equation of motion for the particles. This method is relatively straightforward but inefficient. There is also discussion of implementing current coupling using gyrokinetic particles, in which case the polarization current must be dealt with.

C. STATUS

Currently two state-of-the-art 3-D codes are being supported by the SciDAC Center for Extended Magnetohydrodynamic Modeling (CEMM) project; M3D and NIMROD. These are both focused on the modeling of linear and non-linear phenomena in fusion experiments that require Extended-MHD descriptions.

The NIMROD code solves the primitive form of the plasma fluid-model in axisymmetric toroidal, cylindrical, or periodic-linear geometry with arbitrary poloidal cross-sectional shape. (The geometry must have an ignorable periodic coordinate, but the simulated dynamics are fully three-dimensional.) The user selects which terms are retained in Ohm’s law through an input parameter. The semi-implicit numerical method is used to advance the solution from initial conditions. This avoids severe time step restrictions associated with wave-like normal modes of the system, sound, Alfvén, and whistler waves—while avoiding numerical dissipation. For accuracy at time steps that are orders of magnitude larger than explicit stability limits, the semi-implicit operator for mass motions is based on the linearized ideal MHD energy integral. Matrix inversion is accomplished by parallel preconditioned Krylov methods, which is the most computationally demanding part of the time advance. Performance is therefore dependent on the effectiveness of the preconditioner.

The spatial representation of NIMROD is an important feature of the code. NIMROD uses a combination of logically quadrilateral and triangular finite elements for the poloidal plane and pseudospectral collocation for the periodic direction. The polynomials used for finite element basis functions are selected by the user for optimal efficiency, and poloidal mesh lines need not be orthogonal. For many fusion problems, accuracy is improved by aligning grid lines with the equilibrium flux surfaces inside the separatrix. The grid can also be packed around low order rational flux surfaces to efficiently resolve the small spatial scales that arise at high Lundquist number S . Triangular meshing outside the last closed flux surface allows complicated, realistic boundary shapes.

The M3D code is a parallel code that is especially suited for geometries with inherently three-dimensional boundaries, e.g. stellarators, but can also be used to simulate axisymmetric devices. M3D consists of two parts, a mesh module and a physics module. The mesh module contains the grid, implementation of differential and integral operators, I/O, and inter-processor communication. The physics module handles time advancement of the equations and contains a hierarchy of physics levels that can be invoked to resolve increasingly complete phase-spaces, and therefore provide increasing realism. The module includes resistive MHD, two-fluid, and kinetic particles. Electrons are represented as a fluid with an approximate fluid closure. M3D uses a stream function/potential representation for the magnetic vector potential and velocity that has been designed to minimize spectral pollution. Parallel thermal conduction is simulated with the “artificial sound” method. The solution algorithm is quasi-implicit in that only the most time-step limiting terms including the compressional Alfvén wave and field diffusion terms are implemented implicitly, with explicit time stepping used for the remaining terms.

A three-dimensional mesh is utilized to facilitate the resolution of multi-scale spatial structures, such as reconnection layers and to accommodate fully three-dimensional boundary conditions that occur in stellarators or the evolving free boundary of a tokamak bounded by a separatrix. The mesh uses unstructured, 3-D piecewise-linear triangular finite elements in the poloidal sections. The domain decomposition consists of slicing the toroidal geometry into a set of poloidal planes with each poloidal plane further partitioned into equal area patches. One or more of the poloidal patches are assigned to each processor. The fluid part of each time step consists of uncoupled 2-D scalar elliptic equations that are solved concurrently within each poloidal plane. The PETSc library has been used extensively to provide a portable, efficient parallel implementation for the elliptic equations that need solution at each time step. These are solved with a Krylov accelerated iterative scheme that uses the overlapped Schwarz method for preconditioning. This leads to excellent parallel scalability.

D. CHALLENGES

These codes require high resolution and many time steps to give an accurate representation of modern fusion experiments. To see this, recall that resistivity effects are characterized by a resistive diffusion time scale, $\tau_R \sim \mu_0 L^2 / \eta$, which is much larger than the Alfvén-wave transit time, $\tau_A \sim L \sqrt{\rho \mu_0} / B$. (Here $L \sim 1 \text{ m}$ is the spatial scale of the device). In fusion machines the Lundquist number, $S = \tau_R / \tau_A$, is of the order of 10^8 . As a result, even though resistive effects determine the physics of the process, they actually become important only within some very

narrow layers. Proper resolution of these layers as well as strong anisotropy of plasma properties along and across the magnetic field imposes serious computational challenges.

We can estimate the computational resources required to carry out the necessary simulations for parameters typical of present and proposed experiments as shown in Table A-I.

TABLE A-I. Typical dimensionless parameters for present and proposed experiments

parameter	name	CDXU	NSTX	CMOD	DIII-D	FIRE	ITER
R (m)	Major radius	0.3	0.8	0.6	1.6	2.0	5.0
T_e [keV]	Elec. Temp.	0.1	1.0	2.0	2.0	10	10
β	Plasma beta	0.01	0.15	0.02	0.04	0.02	0.02
$S^{1/2}$	Inv resis. length	200	2600	3000	6000	20,000	60,000
$(\rho^*)^{-1} = Ba/T^{1/2}$	Ion number	40	60	400	250	500	1200
a/λ_e	Recip. norm elec skin depth	250	500	1000	1000	1500	3000

Estimates based on explicit time-stepping with no grid refinement. Let us first estimate the computational requirements for a 3-D calculation with uniform zoning of size Δx and an explicit time-stepping scheme based on the CFL criteria for the poloidal Alfvén wave, i.e. $\Delta t = \Delta x / V_{AP}$. For a 3-D mesh of linear dimension N, i.e., N^3 mesh total mesh points, it would take N time steps to calculate one Alfvén wave transit time $\tau_A = a / V_{AP}$. Typical ideal and resistive MHD instabilities would grow on the timescales $T_{IDEAL} \sim \beta^{-1/2} \tau_A$ and $T_{RESIS} \sim S^{1/2} \tau_A$, requiring about $\beta^{-1/2} N$ and $S^{1/2} N$ time-steps, respectively. Thus, the total number of space-time points required to compute an ideal or resistive instability would be about $\beta^{-1/2} N^4$ (ideal) and $S^{1/2} N^4$ (resistive). The plasma beta, denoted by β , is the ratio of plasma pressure to magnetic pressure. Its value is an important measure of confinement quality.

Current experience shows that with real performance of about 100 Mflops/processor and of order 1000 processor-hours, we can compute a problem with 100^3 mesh points for 10^4 time steps, using a complex fluid model with the compressional wave and field terms implemented implicitly. This is about 10^{10} space-time points in 3×10^{14} operations. This is easily sufficient resolution and time steps to calculate an ideal mode in CDX-U, and is nearly sufficient to study the initial growth phase of a nonlinear tearing mode. We see this since the number of linear mesh points is comparable to: the linear tearing-layer width, $S^{-1/2}$, the ratio of the system size to the ion Larmor radius $1/\rho^*$, and the ratio of the system and the ratio of the system size to the electron collisionless skin depth, a/λ_e . These are the relevant lengths that enter the two-fluid Extended MHD model.

The question is: what type of computer power is needed to study this physics in a larger, hotter device with a stronger magnetic field? We see from Table A-I that depending on what scale length needs to be resolved, the number of mesh points in a linear direction will increase by about an order of magnitude as we go from CDX-U to DIII-D. The increase in the total number of space-time points would be the fourth power of this factor times another scaling factor that will be between unity (for ideal scaling) to about 10 (for resistive scaling). Thus, the number of space-time points required would increase anywhere from 10^4 to 10^5 . Running on a 10 Teraflops

(delivered) computer for 3 days would correspond to about 3×10^{18} floating point operations which would be about 10^4 times greater than what was quoted above for what is available to us today, so a full DIII-D calculation might be feasible with this hardware increase alone.

Grid refinement, implicit time stepping and improved algorithms. It is straightforward to see that the above scaling estimates can be gross overestimates if we take into account improved algorithms and meshing. For example, for a field-line following mesh and with adaptive mesh refinement, the total number of mesh points should only have to grow linearly as we go to larger machines and higher resolution, rather than cubic. With implicit time differencing, the time step will not have to decrease nearly as fast as linear with zone size. More efficient solvers can give an additional factor. Thus, with these computational improvements, some of which have already been implemented to varying degree in M3D and NIMROD, we can realistically expect to be able to calculate modes using Extended MHD models in DIII-D, NSTX, and CMOD in the time frame of this project, and even FIRE and ITER calculations might be within reach. Of course, it also may not be necessary to simulate the exact parameters of a machine if we can determine scaling relations from doing a series of calculations at reduced parameters.

V. PLASMA EDGE PHYSICS AND PLASMA-WALL INTERACTION

A. INTRODUCTION

The edge plasma, which bridges the hot plasma core and the material wall (see Fig. A9) plays a crucial role in both overall plasma confinement and plasma-wall interactions. Some examples of the impact of the edge plasma are:

1. Changes in edge plasma parameters can lead to dramatic improvement in core plasma confinement in the H-mode via the formation of transport barriers, regions with reduced plasma turbulence. The height of the pedestal of this barrier plays a crucial role in the performance of a fusion reactor;
2. Practically all magnetic fusion devices have a density limit, which may be due to strong anomalous plasma transport at the edge;
3. There is a strong, but poorly understood, influence of neutrals and wall conditions on plasma confinement, e.g., one of the best shots in the TFTR tokamak was enabled by lithium conditioning of the walls;
4. Heat load on first wall, which is determined by edge plasma conditions, is a serious issue for reactor-relevant conditions;
5. Wall sputtering, transport of ions and neutrals, including hydrocarbons, in the edge plasma, and deposition processes caused significant accumulation of tritium in the first wall of both TFTR and JET tokamaks.

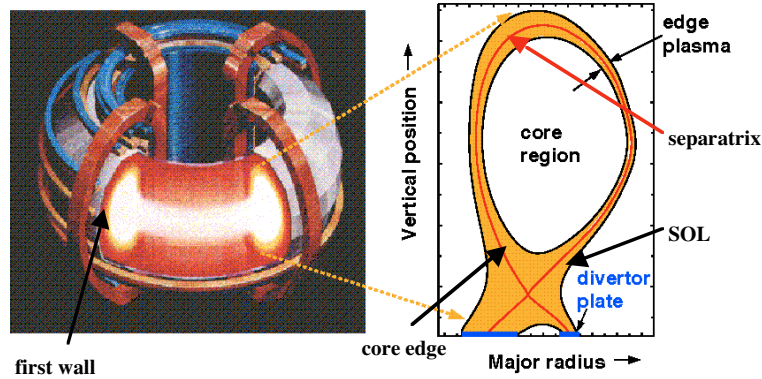


Fig. A9. Schematic view of edge plasma region in tokamak

The plasma edge region has many of the same problems as the core, but it also has a number of attributes that make it crucially distinct from the core. In particular, in toroidal magnetic fusion devices, such as tokamaks, field lines in the core of the device lie, at least approximately, on closed toroidally shaped flux surfaces, giving rise to good confinement of particles and heat. However, on the periphery of such devices, there inevitably exists a *scrape-off layer* (SOL), where magnetic field lines are in direct contact with material surfaces. Due to competition of parallel and perpendicular plasma transport, two-dimensional effects are strong in the SOL. In addition, so-called *divertor configurations* are common to most of the large toroidal devices, in which extra field coils are added to make the magnetic field intersect material surfaces at a location relatively remote from the main plasma volume, as shown in Fig. A9. In divertor configurations the magnetic *separatrix* divides closed magnetic field lines in the core-edge region from open ones in the SOL.

In the core plasma, the separation of scales is both a blessing and a curse. On the one hand, as in gyrokinetic theory, an ordering exists that allows one to solve the equations by averaging over smaller scales and ignoring variations in the longer scales. On the other hand, the same scale separation contributes to the difficulty of a first-principles whole-device simulation. In the edge, by contrast, the spatial scales are compressed, tending to invalidate the ordering schemes. Gyrokinetic ordering, for example, can break down, i.e. $\rho^* \sim 1$, and the collisionality varies along the field from the long mean-free-path to the short mean-free-path regime.

Thus, the solution of the fundamental equations becomes much more difficult, but if solutions are obtained, they should be readily assimilated into the global simulation—or become a microcosm of the global simulation. Indeed, one of the focused integration initiatives (FIIs) might be devoted to this entire region.

B. PROPERTIES OF THE EDGE PLASMA

Plasma near the separatrix, being impacted by fast parallel transport to material surfaces, tends to have steep radial gradients in temperature and density and to be relatively cold. The low temperature, coupled with proximity to bounding surfaces, results in a relatively high concentration of neutral gas and impurities. These properties lead to a relatively strong role for atomic physics processes: ionization, recombination, excitation, and radiative transport.

There is general consensus, supported by both analytic theory and numerical simulations of anomalous transport, that the poloidal $\mathbf{E}\times\mathbf{B}$ flows, spontaneously generated by the nonlinear dynamics, play a central role in regulating the saturation level of the turbulence and the resulting cross-field transport. Strong shear of this poloidal flow tears apart convective eddies and reduces the turbulence level and cross-field transport by forming the H-mode transport barrier. Due to the interplay between significantly different physics on open and closed magnetic flux surfaces, strong shear of the radial electric field and $\mathbf{E}\times\mathbf{B}$ poloidal flow arises, and, as a result, an H-mode transport barrier may be formed somewhat inside the separatrix. Reduction of anomalous transport at the barrier causes steepening of the plasma temperature and density profiles in this region. As a result, strong and repetitive MHD modes can develop causing ELM bursts. It is believed that the MHD modes responsible for ELMs are the so-called ballooning and peeling modes driven by plasma pressure and electric current gradients.

With increasing plasma density, the plasma particle flux to the divertor targets starts to decrease as the *detached divertor regime* is being formed. It is rather well understood and shown with both simplified analytic models and sophisticated 2-D plasma transport codes such as UEDGE that plasma-neutral coupling and atomic-physics effects, including impurity radiation and plasma recombination, play key roles in establishing this regime. However, there are strong indications that cross-field plasma transport also plays an important role here.

Disruption of the discharge for densities above the *density limit* is believed to be due to the mixed effects of enhanced plasma transport to the first wall and thermal collapse of the plasma due to impurity and hydrogen radiation. Interestingly, both the DBM (Univ. Maryland) and BOUT (Lawrence Livermore National Lab.) edge-plasma turbulence codes show trends in plasma transport enhancement at high plasma densities that are somewhat similar to that seen in experiments.

We note that in both improved confinement H-mode and standard L-mode there is rather strong interaction of plasma with first wall material surfaces resulting in both sputtering and (re-) deposition. These are rather complex processes involving ion transport and neutral-particle transport in edge plasmas, chemistry associated with both heavy particle interactions and interactions with electrons, and surface effects (implantation, collision cascades, deposition, adsorption, desorption, diffusion, etc.). In all regimes the first wall is a huge reservoir of hydrogen isotopes, which plays a dominant role in neutral gas recycling.

C. COMPUTATIONAL CHALLENGES AND CODES FOR THE EDGE REGION

Fusion plasmas in general have a large span of spatial and temporal scales, from the electron gyroradius and cyclotron frequency to the device size and the energy confinement time. This large span makes simulation a substantial challenge. In the hot core plasma, there is often a wide separation between the space and time scales characterizing turbulent fluctuations and those characterizing evolution of the equilibrium. This scale separation facilitates the use of separate simulation codes to describe turbulence and transport. However, in the edge region, this scale separation can become small or even non-existent, leading to the challenge of combining a wide range of turbulence and transport scales into a single, large-scale simulation. In addition to the plasma-physics scales, the presence of important atomic physics processes introduces new length

and time scales, which create a range larger than that for the core. Ionization, recombination, and charge-exchange rate coefficients for hydrogen and impurities are in the range of 10^{-14} - 10^{-13} m^3/s , which for typical densities of 10^{20} m^{-3} give time scales of 10^{-6} - 10^{-5} s. On the other hand, near-unity recycling from the hydrogen-saturated material surfaces, where each incident ion results in a neutral hydrogen atom injected back into the edge plasma, yields a long time scale, 10^{-1} s, for establishment of equilibrium profiles.

The edge region of fusion devices generally has substantially lower plasma temperatures than the core, resulting in Coulomb collisional mean-free-paths parallel to \mathbf{B} being much less than the *connection length*, i.e., the parallel distance traveled in making one poloidal revolution. Furthermore, the gradient scale-lengths and observed turbulent wavelengths perpendicular to \mathbf{B} are usually greater than the ion gyroradius. Because of the spatial localization provided by collisions and \mathbf{B} , fluid models have been adopted to give the basic description for both turbulence and transport simulations. However, there is growing concern in the community that fluid models are not adequate for plasma conditions in the H-mode pedestal region, and therefore they should be replaced with more accurate, but much more complex, kinetic models.

The principal edge-plasma turbulence codes within the U.S. community are presently BOUT and DBM. These are 3-D turbulence codes dealing with a fluid plasma description based on the electromagnetic Braginskii equations for plasma vorticity, density, electron and ion temperatures and parallel momentum. The BOUT code is non-local, can describe a magnetic X-point geometry on both sides of the separatrix, and is based on a toroidal segment simulation volume, while the DBM code is a flux-tube code (presently without an X-point) and well suited to parametric studies. With sources added in the core-edge region and sinks in the SOL, BOUT has begun to follow some short-time profile evolution in response to the turbulence.

The numerical algorithms used in BOUT consist of finite-difference equations in 3-D where the resulting ordinary differential equations for the time dependence of each cell variable are advanced with the fully implicit Newton-Krylov solver PVODE. BOUT is written in C. The implicit integration increases the time step by a factor of 3-6 without preconditioning. Parallelization is obtained by domain decomposition in the direction along \mathbf{B} , utilizing MPI for message passing. Because of weak coupling between the domains, scaling with the number of processors is essentially linear up to 120, but using 64 processors is more typical, and simulations have been done on various parallel platforms (IBM SP, T3E, SUN, DEC and Linux clusters).

The DBM code is written in Fortran 90 and solves the reduced Braginskii equations in a general flux-tube magnetic geometry, without (as yet) a magnetic X-point. It utilizes fourth-order spatial finite differencing and a second-order-accurate trapezoidal leapfrog time advance. The communication routines are MPI-based and at present, like BOUT, involve 1-D domain decomposition.

In addition, the edge plasma community has extensive experience with kinetic neutral transport and related atomic physics via DEGAS-2 (PPPL) and TNG (UCSD), as well as the 2-D coupled fluid plasma/neutral transport via UEDGE (LLNL), all of which provide an excellent base for planned extensions. UEDGE is an implicit time-dependent code capable of very long-time simulations of profile evolution that includes the important neutral particle sources from recycling surfaces and gas puffing, plus impurity species.

However, even though there is a consensus that neutrals can be an important ingredient in both edge-plasma turbulence and in the formation of the H-mode barrier, so far edge plasma turbulence codes are lacking the proper physics that would take these effects into consideration.

To describe erosion of the first wall under normal operation conditions the REDEP/WBC package is often used in the U.S. edge plasma community. The WBC is a Monte Carlo code, which computes impurity-atom and ion motion at the kinetic description level, including sputtering and deposition processes, and both elastic and inelastic impurity-plasma collisions. The code is very time consuming to run; therefore it is often run separately, and its output used as input to the REDEP code, which uses cruder models for impurity transport. As an input for plasma parameters the REDEP/WBC package uses either experimental data or UEDGE modeling results. We note that the cross-field impurity-ion transport built into this package is rather rudimentary

VI. EQUILIBRIUM EVOLUTION AND CONFINEMENT

A. INTRODUCTION

Plasma transport or confinement will be a major component of the integrated simulation project. Processes described in the preceding section determine the sources and sinks that drive the plasma fueling, heating, and rotation. In the following section we discuss the confinement or transport mechanisms that balance these. First, however, let us set up the framework in which these operate. With exceptions to be discussed below, the plasma equilibrium consists of nested flux surfaces. Because plasma parameters equilibrate rapidly along the magnetic field, they are nearly constant on these surfaces, and thus transport takes place principally across magnetic surfaces, and can be described in one spatial dimension, denoted by a generalized *radius* or flux label ρ . The term *1-1/2 D transport* refers to the fact that ρ must be related geometrically to the 2-D equilibrium. These *1-1/2 D* transport codes are central to today's efforts at integrated simulation. We will come back to this point later.

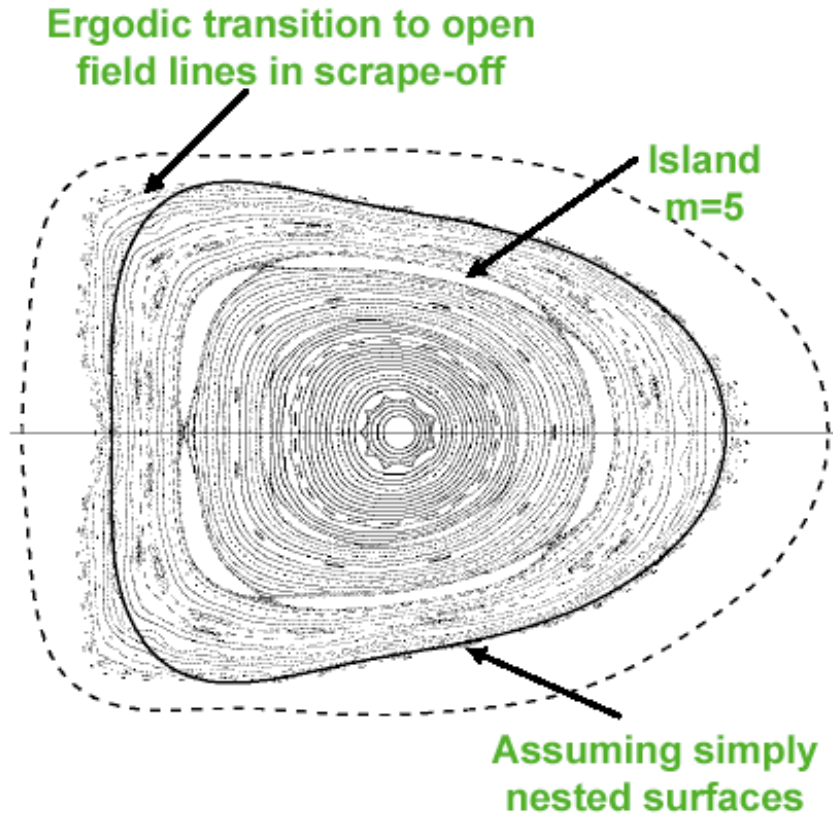


Fig. A10 *PIES equilibrium of a low aspect-ratio stellarator* [Courtesy J. Lyon and W. Houlberg, ORNL].

The breakdown of the above argument gives rise to a physics and computational challenge that will be central to the integration initiative. Islands and ergodic regions can form, owing to MHD instabilities and field errors in tokamaks, as well as in 3-D equilibria in stellarators. Figure A10 depicts a cross-section of a low aspect-ratio stellarator equilibrium showing islands and ergodic regions. (This is a puncture plot with each dot representing the passage of a magnetic field line.) These regions evolve on the transport time scale.

B. TRANSPORT EQUATIONS

Despite these caveats, tokamak transport is reliably described by 1-D surface-averaged transport equations in most circumstances. For stellarators, a design goal is to minimize the externally driven islands and stochastic regions so that similar transport studies are approximately valid.

Construction of a set of 1-D equations makes use of characteristic time scale separation. The fastest or Alfvén time scale ($\sim \mu\text{s}$) is assumed to establish the basic magnetic geometry. This is computed with MHD equilibrium codes that are free from the Alfvén time scale so this timescale is effectively eliminated from the problem. Likewise, particle densities and temperatures are assumed to equilibrate rapidly along the magnetic field lines, so that they can be considered 1-D functions of the flux coordinate function, thus eliminating the fast parallel transport time scale from the problem. The 1-D functions evolve on timescales characteristic of cross-field transport, which is one of the slowest timescales under consideration. This timescale establishes the profiles

of thermodynamic quantities, density, temperature, and angular momentum. Careful selection of variables is required to take advantage of this timescale separation.

The geometry of the flux surfaces is specified by solving the MHD equilibrium equations: $\mathbf{J} \times \mathbf{B} = \nabla p$, $\nabla \times \mathbf{B} = \mu_0 \mathbf{J}$, and $\nabla \cdot \mathbf{B} = 0$. In two-dimensional geometry, appropriate for tokamaks without magnetic islands, flux surfaces are known to exist, and this leads to a nonlinear partial differential equation, the *Grad-Shafranov equation*, for the poloidal *magnetic flux* Ψ as a function of the cylindrical coordinates R, Z in the poloidal plane. Different techniques are used for *fixed boundary* calculations where the plasma/boundary interface is specified, and *free boundary* calculations where the plasma/boundary interface is determined self-consistently from the actual coils that produce the confining magnetic field. In three dimensions, there is an additional complexity in that there is no guarantee that the nested flux surfaces exist. The VMEC 3-D equilibrium code assumes the existence of these surfaces, whereas the PIES 3-D equilibrium code does not.

Figure A5 (or A10), *without* the islands or ergodic regions, is a typical tokamak (or stellarator) result. The radial variable $\rho(\Psi)$ is usually defined in terms of the plasma volume or magnetic flux (integral of $\mathbf{B} \cdot \hat{\mathbf{e}}$ over a surface perpendicular to $\hat{\mathbf{e}}$). For example, $\rho = a(\Psi/\Psi_a)$, $\rho = a(V/V_{\text{tot}})^{1/2}$ or $\rho = a(\Phi/\Phi_{\text{tot}})^{1/2}$, where a is the nominal minor radius of the device, V is the volume and Φ is toroidal flux within a flux surface.

The transport equations themselves are obtained by taking velocity moments of the Boltzmann equation (A-1) and computing appropriate *flux-surface averages*,

$$\langle A \rangle = \frac{1}{V'(\rho)} \int_0^{2\pi} d\phi \int_0^{2\pi} d\theta \sqrt{g(\rho, \theta, \phi)} A(\rho, \theta, \phi), \quad (\text{A-19})$$

$$V'(\rho) = \int_0^{2\pi} d\phi \int_0^{2\pi} d\theta \sqrt{g(\rho, \theta, \phi)}, \quad (\text{A-20})$$

where $V' = dV/d\rho$, g is the Jacobian of the coordinate transformation and A is the function to be averaged. The resulting time-dependent continuity and energy transport equations are of the form:

$$\frac{\partial n_a}{\partial t} = -\frac{1}{V'} \frac{\partial}{\partial \rho} (V' \langle \Gamma_a \cdot \nabla \rho \rangle) + \langle S_{pa} \rangle, \quad (\text{A-21})$$

$$\begin{aligned} \frac{3}{2} \frac{\partial (n_a T_a)}{\partial t} = & -\frac{1}{V'} \left[V' \left\langle \left(\mathbf{Q}_a + \frac{3}{2} T_a \Gamma_a \right) \cdot \nabla \rho \right\rangle \right] - n_a T_a \frac{\partial}{\partial \rho} \left(\frac{\langle \Gamma \cdot \nabla \rho \rangle}{n_a} \right) \\ & - \langle (\nabla \mathbf{u}_a) : \Pi_a \rangle + \sum_{a'} \Delta Q_{aa'} + \langle S_{Ea} \rangle, \end{aligned} \quad (\text{A-22})$$

where $\langle \Gamma_a \cdot \nabla \rho \rangle$ and $\langle \mathbf{Q}_a \cdot \nabla \rho \rangle$ are transport fluxes, $\langle S_{pa} \rangle$ and $\langle S_{Ea} \rangle$ are sources of particles and energy, $\langle (\nabla \mathbf{u}_a) : \Pi_a \rangle$ is the viscous heating, and $Q_{aa'}$ is the energy exchange between species. There are similar equations for momentum balance. Additional constraints are that fast energy

exchange between ions forces their temperatures to be nearly equal and that quasi-neutrality, $\nabla \cdot \mathbf{J} = 0$, determines *ambipolarity* constraints,

$$n_e = \sum_{a=\text{ions}} Z_a n_a, \quad \Gamma_e = \sum_{a=\text{ions}} Z_a \Gamma_a \quad (\text{A-23})$$

The fluxes, viscous heating, and sources are inputs to the code and are discussed in more detail in the preceding and following Appendices. Kinetic theory is used to provide *closure*, whereby Γ_a , \mathbf{Q}_a , and Π_a are expressed in terms of the thermodynamic variables n_a , T_a and their gradients. For example, the particle flux is usually expressed in the *diffusive-convective* form

$$\langle \Gamma_a \cdot \nabla \rho \rangle = -\langle |\nabla \rho|^2 \rangle D_a \frac{\partial n_a}{\partial \rho} + \langle |\nabla \rho|^2 \rangle^{1/2} n_a u_{na}, \quad (\text{A-24})$$

$$\langle \mathbf{Q}_a \cdot \nabla \rho \rangle = -\langle |\nabla \rho|^2 \rangle n_a \chi_a \frac{\partial T_a}{\partial \rho} + \langle |\nabla \rho|^2 \rangle^{1/2} n_a T_a u_{qa} \quad (\text{A-25})$$

where $\langle |\nabla \rho|^2 \rangle$ is a geometrical factor, D_a and χ_a are the particle and heat diffusivities, and u_{na} and u_{qa} are the convective velocities. The latter may themselves be represented in terms of other plasma gradients and referred to as *off-diagonal elements*.

The magnetic fluxes also evolve. This is typically described in a Grad-Hogan scheme, in which the toroidal flux is taken as the reference frame and is updated with infrequent calls to the MHD equilibrium equation. The poloidal flux evolves relative to the toroidal flux and is described by resistive diffusion, making use of Faraday's law (see Eq. (A-3)) and Ohm's law in a flux function form that relates the toroidal current density as the secondary of a transformer to the external loop voltage. The time scale is governed by the parallel electrical resistivity.

C. USES OF TRANSPORT CODES

Codes that solve the transport equations as described here form the core of current state-of-the-art integrated modeling. These codes have proliferated over the years to serve a multitude of purposes, and each achieves good results within its range of validity. We distinguish two basic modes of operation. In the *interpretive* mode, all (available) plasma-parameter profiles and their time derivatives are inferred from experimental data, including the equilibrium geometry, which is calculated in an MHD code using magnetic data as constraints. The sources, such as energy deposition, are likewise calculated using the measured profiles. The code then solves (A-21) and (A-22) to calculate the transport fluxes or diffusivities, Eqs. (A-24)-(A-25), which are used to determine empirical confinement scalings and the like. In the *predictive mode*, on the other hand, models for the diffusivities or fluxes are employed, and the code calculates the time evolution of Eqs. (A-21) (A-22) to determine the plasma profiles, which can then be compared with experiment.

The major interpretive codes in use today, TRANSP and ONETWO, contain detailed models of all the principal sources and sinks that are relevant to tokamaks. Each can be run, alternatively, in the predictive mode. Indeed, in the absence of one or more pieces of

information, a subset, such as the current or poloidal-field evolution, may be simulated within an interpretive run.

Other codes, such as BALDUR, WHIST, CORSICA, or TSC, are simulation codes whose main use is testing transport models or performing design studies. These carry varying levels of detail outside the particular feature being tested. For example, a core thermal-transport model may be tested by running only the temperature evolution equation, holding the density fixed, setting a boundary condition just inside the edge, and taking the source as calculated in an experimental interpretive run. The goal would be to test the temperature profile evolution without complicating distractions. Similar simulations in which all of the density, temperature, and momentum equations for each species plus current penetration could be run, while still using simple boundary conditions. At the other end of the spectrum, one might wish to explore reactor designs, studying wall conditions, connection to external circuits etc., while employing a very simple plasma model based on empirical scaling. Each of these problems requires different functionality in the code to make efficient use of the available computer time.

D. CHALLENGES OF TRANSPORT MODELING

Flexibility. A principal challenge of the simulation initiative is to preserve present functionality within a flexible configuration that allows the user to select from the full range of options and efficiently run his/her case, from the very simplest model to the most detailed full integration.

Rotation and radial electric field. The radial electric field, poloidal and toroidal rotation, and the pressure gradient are all coupled through the radial force balance. Both the physics and the computation of these processes require continued development and will form an essential aspect of integrated simulation. For example, bifurcations are observed experimentally, in which the plasma jumps suddenly to an alternate state, often forming a transport barrier. Enhanced diagnostics and developing theoretical models imply scenarios in which sheared $\mathbf{E} \times \mathbf{B}$ flow suppresses turbulence, while turbulence can drive locally sheared poloidal rotation. Also, $\partial E_\rho / \partial \rho$ squeezes orbits and reduces collisional transport, while toroidal rotation enhances MHD stability. Toroidal rotation generally appears diffusive and governed by turbulent transport but can appear even in the absence of apparent torque. Other issues are whether we should treat E_ρ or poloidal rotation as the independent variable, and whether we can express bifurcation threshold conditions in terms of macroscopic quantities. Internal barriers are strongly localized and move in time, indicating the need for dynamic gridding algorithms for better resolution. Finally, in stellarators, the ambipolarity constraints are expected to govern E_ρ , and in tokamaks, broken toroidal symmetry can do the same.

Transport in the edge and SOL. The basic equations in the edge and SOL are much the same as in the core, but the computational challenges are even greater. Physics and computational challenges include formulation of both turbulent and collisional transport models in steep gradient regions, formulation of the coupling/transition between the closed field lines (slow radial transport timescale) and open field lines (faster parallel timescale), and accommodation of multiple timescale phenomena e.g., *edge localized modes* (ELMs) of the H-mode layer. (See Sec. VIII.)

Non-nested surfaces. Finally, one of the most difficult challenges of integrated core modeling is to extend all the considerations of this and the adjacent two sections to take into account the islands and stochastic regions illustrated in Fig. A10 .

VII. EXTERNAL SOURCES

A. INTRODUCTION

External systems that add mass, momentum, or energy to a plasma are essential tools in the successful efforts to obtain good performance both in present experiments and in any future experiments and reactors. At present, the external sources include beams of neutral atoms that can carry energy, particles, and angular momentum across magnetic fields; radio frequency waves (RF) whose interactions with a plasma can be used for heating, current drive or flow drive; high-speed pellets of frozen fuel gas that can deliver particles deep into the plasma core; and gas fueling which supplies particles to the plasma edge. In a burning plasma experiment or reactor, the fusion-produced alpha particles, which have some properties in common with beam-injected particles, will provide the principal energy source.

External sources are important, not only to provide fuel (D and T in a reactor) and energy (heating the plasma to 10 keV or more), but also to provide essential elements of control. The plasma current, pressure, and rotation-velocity profiles all are crucial to plasma performance and can be influenced by these sources. We also have sources such as impurities and gas from plasma-facing components, which can have undesirable consequences, as well as losses from radiation.

The computational capabilities related to neutral beam injection are very well developed and are presently integrated into many codes. The work could be easily ported to codes developed in new initiatives. Wave-plasma interactions at RF frequencies (from ion to electron cyclotron frequencies) are the subject of intense ongoing research including fusion SciDAC activity. However, the scope of needed work, and the ability to provide interactive coupling with other plasma codes, extend far beyond the SciDAC activity. This area includes many distinct problems and will be an essential element of future plasma prediction, interpretation, and control schemes. Work on the ablation and subsequent transport and deposition of fuel from injected pellets is in a relatively early phase of development but certainly amenable to computation. However the physics of fueling in general is not in a satisfactory state at present and would benefit from basic theory studies of particle transport.

B. NEUTRAL BEAM INJECTION

A number of well understood physics processes are involved in neutral beam injection (NBI) at energies in the neighborhood of 100 keV. The capture of neutral atoms by ionization and charge exchange is modeled by Monte Carlo calculations. A thermal neutral atom formed by charge exchange may escape or be re-ionized. The orbits of fast charged particles are followed and their slowing down and scattering are computed in a Fokker-Planck model solved by Monte Carlo. Secondary processes such as re-neutralization of energetic ions by charge exchange are also calculated.

For tokamaks the TRANSP neutral injection package is the most widely used. It has recently been extracted from the integrated interpretive modeling code TRANSP as a separate module for the National Transport Code Collaboration (NTCC). See the web site <http://w3.pppl.gov/NTCC/NUBEAM/UserGuide>. Much of interface code is automatically generated by Python script. Input and output is passed in f90-derived data types, employing internal 2-D flux coordinates (ρ, θ) , where ρ is the normalized minor radius, and θ is the poloidal angle (the short way around in Fig. III.1 of the main report). Outlines for conversion among other common coordinate representations are included. Inputs consist of MHD equilibrium quantities (magnetic field geometry, plasma pressure in space), profiles of density and temperature of a large number of particle species, descriptions of injected neutral beam geometry and characteristics, atomic physics data and cross sections, wall geometry, and controls for code operation and inputs to auxiliary models. Outputs are radial profiles of power deposition, driven current, ion/electron source rate, and rotation, 2-D profiles of neutral and fast ion density, and the fast ion distribution in four phase-space dimensions $(\rho, \theta, E, v_{||}/v)$.

The issues for this kind of modeling are more computational than physics: increasing speed, increasing resolution in space and velocity space, and extension to 3-D equilibria for stellarators and other non-axisymmetric configurations.

An entire separate field of study, however, concerns possible instabilities driven by populations of high-energy particles. These are seen experimentally and considerable progress has been made in explaining the observations by theory and computation. These are important because they can lead to anomalous losses of fast particles and reduce heating efficiency.

Alpha particles produced at 3.5 MeV in D-T fusion reactions have many of the properties of high-energy beam particles, resulting in *alpha heating* and including the prospect of driving instabilities, and can be modeled similarly. The chief differences are the much higher alpha energies and their isotropic initial distribution. Because large numbers of alphas will not be produced until a burning plasma is actually achieved, it is extremely important to include this physics in our integrated computation and in this way anticipate burning plasma performance.

C. EDGE PARTICLE SOURCES

Modeling of edge particle sources is a discipline unto itself and must be included in the edge plasma studies. (See Sec VIII.) Edge conditions in fusion devices have a tremendous influence on the bulk plasma behavior. Neutral particles in the edge also influence other physics processes besides fueling. For example, charge exchange of plasma ions with edge neutrals exerts torque affecting plasma rotation, and neutrals participate in edge instabilities. Edge particle sources are inherently three-dimensional. Several modeling codes presently exist. Most are completely 3-D Monte Carlo (EIRENE, DEGAS). A fast neutral code (NUT), based on zonal integration has recently been placed in the NTCC module library.

D. RADIO-FREQUENCY WAVE HEATING AND CURRENT DRIVE

Besides inductive Ohmic heating, common to all tokamaks (but usually absent from stellarators), there are three important wave frequency regimes to consider, each associated with a particle or plasma resonance. These are:

- *Electron cyclotron range of frequencies* (ECRF), $\omega \approx \omega_{ce}$.
 $f \sim 100$ GHz ($\tau \sim 10^{-11}$ sec), $\lambda \sim 0.3$ cm, where λ is the wavelength. The launcher is far from the plasma; the waves propagate in free space and can be computed with geometrical optics.
- *Lower hybrid range of frequencies* (LH), $\omega_{ce} \ll \omega \ll \omega_{ci}$.
 $f \sim 0.5 - 5$ GHz ($\tau \sim 10^{-10}$ sec), $\lambda \sim 1$ cm. The launcher is near the plasma; the waves do not propagate in vacuum but are usually computed with geometrical optics.
- *Ion cyclotron range of frequencies* (ICRF), $\omega \approx \omega_{ci}$
 $f \sim 100$ MHz ($\tau \sim 10^{-8}$ sec), $\lambda \sim 10$ cm. The launcher is near the plasma, the waves do not propagate in vacuum, and they require solution of wave equation. Alfvén waves at frequencies $\omega \ll \omega_{ci}$ have also been considered for heating and current drive.

Waves can have strong interactions at localized regions in space due to various kinds of resonance. Either the wave velocity matches the particle velocity $v_{wave} = \omega/k = v_{particle}$, and the particle sees a steady, accelerating electric field, or the wave frequency in a frame moving with the particle (Doppler effect) matches a harmonic of the particle cyclotron frequency, $\omega - kv_{particle} = \ell \omega_c$, and the gyrating particle sees a steady component of the electric field. The effect is an energy and momentum kick each time the particle passes through resonance. These kicks accumulate over time to produce energy gain and directed velocity resulting in bulk plasma heating, very energetic tail populations, electric current and fluid drift or flow. In Fig. A5, we have shown a tokamak cross-section with schematic launchers, a wave, and a resonance layer. (Also depicted is a chain of magnetic islands. See Sec. IV.) Similar resonances also occur throughout the plasma when spontaneous turbulence arises.

This illustrates an important difficulty in solving the basic equations, Eqs. (A-1)-(A-3), namely that for perturbations from equilibrium, *the distribution function $f_a(\mathbf{x}, \mathbf{v}, t)$ can be highly structured, requiring very fine resolution in some regions of both configuration and velocity space.*

Let us consider the full-wave calculations as they apply, for example to ICRF heating at frequency ω . The wave propagation and plasma response are described by Eqs. (A-1)-(A-5) with displacement current included. We have now returned full circle to the highest frequency ranges of the whole integrated simulation. For this problem, we exploit the separation of time scales and the small amplitude of the waves to linearize the fields $\mathbf{B}(\mathbf{r}, t) = \mathbf{B}_0(\mathbf{r}) + \mathbf{B}_1(\mathbf{r})e^{-i\omega t}$, $\mathbf{E}(\mathbf{r}, t) = \mathbf{E}_1(\mathbf{r})e^{-i\omega t}$, and apply the *quasi-linear* method of solution to the plasma response for each species, $f_a = f_0 + f_1 e^{-i\omega t} + f_2$, where f_1 is the fast response producing the wave current \mathbf{J} in Eq. (4.4), and f_2 is the slow time scale response that gives the power deposition and equilibrium evolution. We give a schematic representation of the equations, in which the fast part of Eq. (A-1) reduces to

$$i\omega f_1 + L_1\{f_1\} = L_2\{\mathbf{E}_1, f_0\} + L_3\{\mathbf{B}_1, f_0\}, \quad (\text{A-26})$$

where L_1 - L_3 are complicated *linear* operators. The slow background response then is the solution to

$$\frac{\partial f_2}{\partial t} + L_1\{f_2\} = Q_1\{f_1, \mathbf{E}_1\} + Q_2\{f_1, \mathbf{B}_1\} + C(f_2), \quad (\text{A-27})$$

where Q_1 and Q_2 are *quadratic* or bi-linear operators, proportional to $f_1\mathbf{E}_1$ and $f_1\mathbf{B}_1$, where only the “zero-frequency” components are retained. The set is completed with boundary conditions that connect to the vacuum region and antennas that drive currents $\mathbf{J}_{\text{ant}}e^{-i\omega t}$. To solve these equations, a spectral representation is employed in which the plasma is treated as locally uniform with Fourier expansions in three dimensions.

The wave code with the least restrictive approximations is the All Orders Spectral Algorithm (AORSA). Discretizing using the method of collocation yields equations for the Fourier amplitudes, a gigantic, dense linear system. On the NERSC computer SEABORG, a 3,000-processor IBM SP, a typical run requires 8 hours of processor time at approximately 1.7 teraflops, and memory of 750Mbytes/processor or 1,200 Gbytes total. Inputs are the MHD equilibrium quantities (magnetic field geometry, plasma pressure in space), profiles of density and temperature of a large number of particle species, distribution functions for non-Maxwellian species (slowing-down distributions or superpositions of Maxwellians), and wave parameters, descriptions of antenna geometry etc. The outputs are Fourier amplitudes of wave fields and plasma response obtained by post-processing: profiles of power deposition, driven current etc., obtained from the moments of f (evolution of $f_0 + f_2$). Calculating wave sources is in itself a task of integrated modeling, as this background evolution, on the same time scale as transport processes, in turn affects the wave absorption. This full integration in calculating wave sources is not presently achieved. A SciDAC project is making progress on integration, but the scope is far short of what is needed

E. SUMMARY: THE ROLE OF SOURCE MODELS IN COMPREHENSIVE INTEGRATED SIMULATION

For whole device modeling, source models covering a range in levels of description will be essential elements of any comprehensive device model. We need a 3-D solution of the drift kinetic equation including RF effects, radial transport, and finite orbit width effects.

In focused integration initiatives, source modeling will be essential. A few examples are:

- Particle source modeling is already a key element of edge studies. There are strong interactions between the edge plasma and RF launching structures – RF fields perturb the edge plasma, and edge plasma characteristics influence the wave spectrum launched. This requires integration of RF models (particularly the antenna model) with an arsenal of edge modeling codes.
- In island formation, heating by RF waves at rational surfaces and energetic particles produced during RF heating can stabilize island growth. RF driven currents can either stabilize or destabilize island growth. This requires integration of RF models with MHD and transport near the island (See Sec. VII).

- To understand the role of radial electric fields on transport and flows in stellarators, we need 4-D or 5-D solution of the drift kinetic equation including RF effects.

VIII. FUSION SIMULATION PRESENT CAPABILITIES STATUS

This section summarizes the current status of integrated computational modeling and simulation of toroidal confinement fusion systems. The intent in this section in the present document is to provide a general perspective of the status of this very active and mature field. This section responds to the explicit request in the subcommittee's charge letter to report on the status of fusion simulation capabilities, and is the context from which the FSP is defined. The present fusion simulation capabilities form a significant part of the critical underpinning of the FSP.

There are over 50 major toroidal physics design and analysis codes being maintained by the magnetic fusion community. The major multi-user codes are depicted in Figure A11, which shows how they divide into groups, and indicates with arrows the flow of information from one code group to another.

The axisymmetric free boundary equilibrium codes solve the force balance equation by calculating the poloidal magnetic flux in cylindrical coordinates for given pressure and current profile parameterizations. These can be used to define the boundary for the inverse equilibrium codes. There are also two major fully 3-D equilibrium codes in use: VMEC, which assumes the existence of good magnetic surfaces *a priori*, and works in a coordinate system based on these, and PIES, which calculates the existence of surfaces as part of the solution, if they exist.

The collection of linear macroscopic stability codes maintained by the MFE community is quite mature and can assess the stability properties of a given equilibrium with respect to both ideal and non-ideal (resistive) MHD, including the effects of an energetic particle component.

Major U.S. Toroidal Physics Design and Analysis Codes

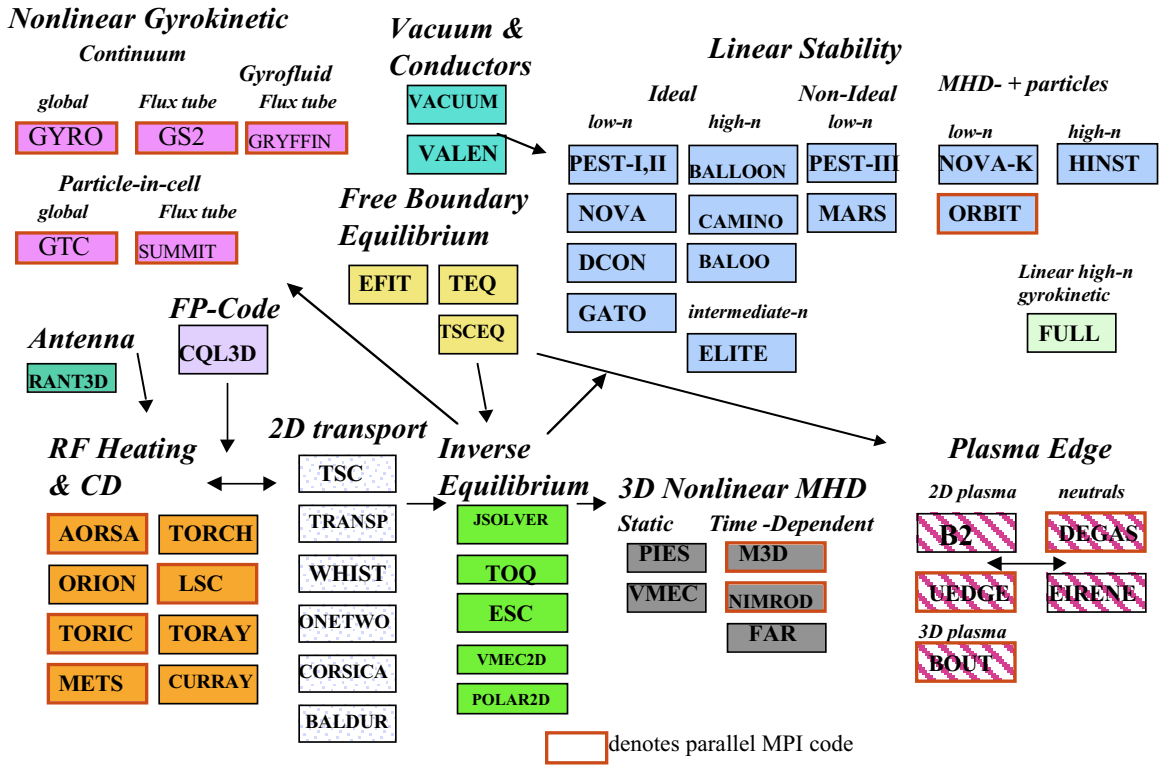


Fig A11. Major U.S. toroidal physics design and analysis codes used by the plasma physics community.

The nonlinear codes fall into four major groupings. In descending order of the frequencies addressed, these are the: 1) RF Heating and Current Drive codes, 2) the Nonlinear Gyrokinetic codes, 3) 3-D Nonlinear Extended MHD codes, and 4) the 2-D Transport codes.

The RF Heating and Current Drive codes calculate the propagation of electromagnetic waves of a given frequency through prescribed background plasma, including reflection and absorption. The codes are of two major types: ray-tracing (or geometrical optics), and full wave (global solution). There are also depicted antenna and Fokker-Planck codes, which are closely coupled with the RF codes, and provide boundary conditions and background distribution functions. The RF codes are designed to calculate the instantaneous heating and current-drive profiles for a given plasma equilibrium subject to a given RF oscillator source and antenna.

The gyrokinetic codes are based on an analytic reduction of the full 6-dimensional plus time plasma distribution function obtained by averaging over the rapid gyro-motion of ions in a strong magnetic field, and by neglecting the displacement current in the Maxwell equations to remove “light waves” from the system. These codes are appropriate for studying 3-D turbulent transport in a background system with fixed profiles.

The 3-D nonlinear Extended MHD codes are based on taking velocity moments of the Boltzmann equation to yield 3-D magneto-fluid equations for the evolution of the average plasma velocity, density, and pressure, along with a closure procedure. These codes are appropriate for describing global stability phenomena such as sawteeth oscillations, magnetic island evolution, and plasma disruptions.

The 2-D transport codes presently form the core capability in our community for integrated modeling. There are six major codes, with considerable overlap, that exist largely for historical reasons. These codes are all based on the Grad-Hogan evolving equilibrium description where the inertial terms in the momentum equation are neglected and the remaining MHD equations are averaged over the flux surfaces, where they exist.

The 2-D transport codes are all very modular. They are each a collection of equilibrium modules, transport modules, solvers, and source and sink modules representing Neutral Beam Injection (NBI) and RF heating, pellet and gas injection, impurity radiation, and the effects of saturated MHD activity such as sawteeth and islands. These codes have recently benefited from the National Transport Code Collaboration (NTCC), which has formed a modules library so that modules taken from individual codes can be exchanged and shared (see, e.g., w3.pppl.gov/NTCC for more details on this). While these codes address integrated modeling, the individual modules represent simplified reduced descriptions of the full three-dimensional physical phenomena being modeled.

A summary of these four major code groups and the timescales being addressed by them has been given in Fig. A6. The RF codes address frequencies of order the ion cyclotron frequency, Ω_{ci} , and above, up to the electron cyclotron frequency Ω_{ce} . (Again, recall the interchangeable notation for these two quantities, ω_{ci} and ω_{ce} .) The gyrokinetics codes typically take time steps about 10 times longer than the ion cyclotron frequency, whose motion is analytically averaged over, and are normally run for 10^3 to 10^4 time steps to calculate stationary turbulent fluctuation levels. Recent additions to these codes to include some electron timescale phenomena bring in the electron transit time, which lowers the maximum time step. The Extended MHD codes need to resolve phenomena occurring on the Alfvén transit time, τ_A , although most codes are at least partially implicit to avoid a strict restriction on the time step based on this. These codes can normally run 10^4 to 10^5 time steps to address MHD phenomena such as sawteeth and island growth. The 2-D transport codes are very efficient and can take many long time steps to model the entire discharge. However, the 2-D edge transport codes need to resolve the parallel dynamics and use a time-step based on the parallel sound-wave propagation near the edge region.

The calculations now being performed with the gyrokinetics codes, the Extended MHD codes, and the RF codes, are straining the limits of the existing computing capabilities and capacities. For example, recent attempts by the core-turbulence gyrokinetics codes to include both electron and ion dynamics in a self-consistent simulation require upwards of 10^4 processor-hours (over one processor-year) on the IBM SP3 at NERSC to generate one result for a set of fixed background profiles. Similar times are required by the Extended MHD codes to calculate the growth and self-consistent saturation of a neoclassical tearing mode. Thus, we can take solace in the fact that the capability is mostly in place, but must deal with the fact that the computational requirements for a fully integrated 3-D comprehensive simulation capability are truly daunting.

Examples of fundamentally important experimental phenomena that involve 3-D physical processes that cross theoretical boundaries and thus cannot adequately be addressed by the present suite of above-described codes include:

Pedestal physics – A description of the transport barrier that forms in the region of the plasma between the core and the edge, and of the associated edge localized relaxation events;

Long time scale profile evolution – A way to self-consistently evolve the global profiles of plasma temperature and density on the energy-confinement time scale from turbulent transport and in the presence of magnetic islands and other MHD phenomena.

Edge transport: A description of long-mean-free-path particle and heat transport outside the closed magnetic flux surfaces, on the open field lines that impact the first wall or divertor and involve multi-phase physics

Self-consistent heating and current drive: A fundamental model of the interaction of Radio Frequency (RF) waves with plasma in the presence of plasma turbulence.

Sawtooth phenomena – Internal MHD-type modes in the hot core of tokamak plasmas for which fast ion and kinetic effects are clearly relevant experimentally but are only beginning to be addressed computationally.

Island physics: incorporation of the effect of 3-D island formation on equilibrium evolution and turbulent transport

These are but some of the important problems to be addressed by the integrated simulation initiative.

IX. FOCUSED INTEGRATION INITIATIVES – CHALLENGES AND OPPORTUNITIES

The following Subsections A-D expand upon the descriptions of the candidate focused Integration Initiatives (FIIs) described in the main text. These are based on reports from working groups at the September 23-24, 2002 Community Workshop, each concentrating on a particular FII.

A. PLASMA EDGE

The boundary or edge-plasma of fusion devices plays a vital role in their operation. The edge-plasma region is generally considered to be the region where substantial two-dimensional (2-D) or 3-D variations can occur in the plasma, neutral particle, and magnetic equilibrium quantities. In addition, owing to the lower plasma temperature and proximity to material surfaces: neutral gas, sputtered impurities, and atomic line-radiation can become important components. Thus, a rich variety of potential interactions can take place in this region.

The ISOFS edge discussion group identified four elements that are key to successful operation of an MFE fusion device:

- (1) predicting conditions and properties of the pedestal energy transport barrier just inside the magnetic separatrix;

- (2) understanding plasma/wall interactions for particle recycling and wall lifetime from high energy fluxes;
- (3) controlling tritium inventory including co-deposition; and
- (4) controlling wall impurity production and transport into the plasma.

A number of models of varying sophistication exist to describe these processes. Some models already provide a level of coupling, e.g., hydrogen transport, recycling neutrals, impurity sputtering, and impurity transport codes. However, many of the constituent models need improvement, and much more inclusive couplings are required to self-consistently predict the edge-plasma behavior.

In setting priorities for the edge region, it was felt that the short-term (five-year timescale) work should focus on a better understanding of what controls the suppression of plasma turbulence to produce a transport barrier in the pedestal region (#1 above), and its associated impact on plasma profiles. The ability to predict the behavior of the edge pedestal barrier is essential for projecting the net fusion output of MFE devices as discussed extensively at the Snowmass 2002 Fusion Study Workshop. Presently, the key parameter that is believed to control the core fusion output is the plasma temperature at the top of the pedestal; this parameter is now either extrapolated from existing experiments or assumed.

The development of a predictive model of the pedestal requires two key advances. The first is the inclusion of kinetic effects in the 3-D turbulence simulations such that the physics model can span the region from the nearly collisionless portion at the core side of the pedestal to the more collisional region near and outside the magnetic separatrix. Presently, turbulence codes fall into two classes: one class is the collisional fluid codes allowing three spatial dimensions and including the strong magnetic shear region in the edge; the other class is the kinetic particle or continuum codes using three spatial and two velocity-space dimensions to capture the physics of plasma with long mean-free paths, but allowing only very simple plasma geometry. These codes are very compute-intensive, requiring parallel computers with run times of many hours or days (> 2000 node-hours). The computational challenge here is to obtain a generalized code or coupling of codes that can treat the full range of collisionality through the pedestal for geometries relevant to the plasma edge.

Another component needed for the pedestal is the description of periodic edge profile relaxations called Edge Localized Modes (ELMs), which are believed to be caused by long wavelength MHD instabilities. The transport barrier is intermittently interrupted by these modes. The peak heat flux to material surfaces from such events is a serious concern for a reactor-sized device. Inclusion of such modes in the microturbulence codes should be considered, but requires a larger spatial mesh and an extension of the physical model to capture this MHD phenomenon. An alternative approach is to use a separate code for the turbulence from MHD modes, or to use a linear stability code to enforce marginal stability of the plasma pressure profile for long-time transport evolution.

A second key advance thought possible in the five-year time frame is to couple the turbulent plasma fluxes with a transport calculation of the profile evolution. Such coupling is the heart of a predictive model. This is the plasma-edge analogue of the “Turbulence on the Transport Timescale” FII described in the next section. The turbulence drives plasma fluxes that, together

with sources such as neutral ionization, largely determine the plasma profiles; since these plasma gradients provide the free energy to drive the turbulence, it is essential that the turbulence and profile evolution be coupled together. Plasma-wall interactions of sputtering and recycling can make the profile evolution time substantially longer than the turbulence saturation time. Devising stable and efficient coupling schemes is a major task here, which may have spin-off to related couplings for other regions of the fusion plasma and beyond. Experiments and turbulence simulations often show large, intermittent transport events that need to be properly characterized.

Beyond the five-year time frame, edge-plasma modeling should work to develop and couple more detailed models of the plasma-wall interactions. These include models for sputtering, recycling and re-deposition, and transport of neutral gas impurities and radiation. In addition, the edge model should look inward to couple with core physics inside the pedestal region. A vision is that a successful edge model could eventually incorporate the core region models for a whole-device simulation.

B. TURBULENCE ON TRANSPORT TIMESCALES

The nature of the problem to be considered can be summarized as follows: The “anomalous” transport of mass, energy, and angular momentum in toroidal MFE devices is dominated by fluxes driven by plasma turbulence. There is a significant disparity of scales, especially timescales. This is a highly coupled system: the plasma pressure and densities are very nearly constant on magnetic flux surfaces, and can thus be considered to be one dimensional (1-D) functions of the flux coordinate ψ ; one-dimensional transport equations can be constructed to describe the evolution of these profiles, whose gradients drive turbulence, while the turbulence (3-D, anisotropic) produces the fluxes that drive the evolution of these 1-D profiles.

The object of this Focused Integration Initiative (FII), is to bridge the range of temporal and spatial scales so as to compute the above coupled system self-consistently, *as opposed to* just computing 3-D fine-scale turbulence with fixed background profiles, or computing 1-D transport with highly reduced theoretical or empirical models of the turbulent fluxes.

The single overarching science issue and goal is the self-consistent calculation of global confinement from first-principles physics. The initial (easier) focus would be to determine steady-state confinement; following time evolution on the transport timescale is conceptually no more difficult but is more computationally demanding. The achievement of the steady-state goal would, as a side benefit, enable optimization studies. Important issues like simulation of both steady-state and time-dependent versions of internal transport barriers are subsets of the overall goal.

There are a number of candidate approaches for achieving the goal. These include:

- (1) direct coupling of the transport and turbulence equations;
- (2) an expert system working together with a smart database of past turbulence simulation results and/or analytic models for transport coefficients, which detects when transport has moved outside of the domain of applicability of the database and triggers new turbulence simulations to extend the domain of applicability;

- (3) developing a viable gyrofluid closure and directly integrating the resulting fluid equations; and
- (4) projecting long-timescale evolution from moments of the extrapolation of particle weights in a gyrokinetic particle-in-cell code.

This candidate FII entails many disciplines in physics and computation. It also entails a number of generic integration issues, including: coupling of disparate timescales; coupling of descriptions with different dimensionality; interfacing to experiments for validation; the need for a flexible framework/environment to support experimentation with multiple approaches; visualization; expert systems to detect failure of an integration component; software standards; and database management. All of these issues present opportunities for collaboration between the theoretical/computational plasma physics and the computer science/math communities.

Such an initiative would also need a strong theory component. Most importantly, there needs to be a parallel effort in analytic turbulence theory to provide crosschecks and understanding. Theory will also be needed for the gyrofluid approach and other formalism extensions, and for development of synthetic diagnostics.

There are clearly opportunities for further linkages and progress toward a full integrated simulation. Turbulence and MHD dynamics may need to talk to one another directly as opposed to via the intermediary of a transport code, but this coupling may be a logical extension of the transport-turbulence coupling activity, as the necessary flows of information are similar. Another logical extension is coupling of the turbulence equations to real sources. But, perhaps most importantly, if the transport-timescale part of transport-turbulence coupling is handled by an existing or new (developed under the initiative) full-device integrated modeling/transport code, this activity immediately has access to many other developments in whole-device integration.

C. GLOBAL STABILITY

Global stability issues play a central role in determining the optimal operating regime of fusion devices, and in describing their time evolution. It is well known that under some operating conditions, an experimental discharge can spontaneously transform from a symmetrical stable system exhibiting good confinement into one that exhibits symmetry-breaking oscillations and poor confinement or becomes unstable and disruptive. These events are known as sawtooth oscillations, Neoclassical Tearing Modes (NTM), disruptions, Edge Localized Modes (ELMs), or Resistive Wall Modes (RWM), among others. The predictive calculation of the onset and evolution of these events is the over-arching scientific question in this FII.

The long time evolution of tokamak discharges is often described by nested magnetic flux surfaces and two-dimensional axisymmetric force balance coupled with diffusive transport of the one dimensional surface averaged thermodynamic and field quantities. The transport coefficients used in the diffusive model are typically analytic approximations to the results of three-dimensional, sub-grid-scale turbulence that is described by kinetic theory. The properties of the turbulence are determined by the axisymmetric plasma profiles, which in turn are affected by the transport coefficients. The first-principles coupling of the transport and kinetic turbulence

models is a formidable problem requiring integrated modeling as described in the previous section.

However, the force balance assumed in the transport model can occasionally become unstable and yield dynamics that evolve on an intermediate time scale that is much shorter than the transport time scale, but much longer than the time scale of the kinetic turbulence. These motions result in three-dimensional magnetic perturbations that break both the underlying axisymmetry of the overall configuration and the nested topology of the magnetic field. Their nonlinear evolution can strongly affect the confinement properties of the magnetoplasma system, and can re-arrange the plasma profiles on time scales faster than that described by diffusive transport.

At relatively low temperatures, these dynamics are well described by *resistive magnetohydrodynamics* (MHD), a mathematical model in which the plasma is treated as an electrically conducting fluid subject to electromagnetic body forces. Solutions of this model are complicated by a wide separation of space and time scales, and by the inherent high degree of anisotropy that occurs in a magnetized plasma. At the higher temperatures that occur in modern tokamaks, kinetic effects both parallel and perpendicular to the magnetic field introduce important physical processes that can affect the global MHD evolution of the plasma. The challenge is to develop mathematical and computational models that include these kinetic effects while retaining the computational tractability of the fluid model. Such models are collectively called *extended MHD*.

There have been two approaches to developing extended MHD models, as described in Section IV. One is to take analytic moments of the higher dimensional drift kinetic equation to obtain expressions for the higher order fluid *closures* (e.g., the heat flux and the components of the stress tensor) that capture the kinetic effects within the fluid model. The other is to solve the kinetic equation by sub-cycling within a time step of the MHD model. Velocity moments of the resulting distribution function can be taken numerically to calculate the required closures. While this approach may be sufficient for minority (or possibly even majority) ion species, it is difficult to envision it being applied to electron dynamics because of their small mass and rapid dynamics. There it is likely that we must continue to rely on analytic closures.

A full modeling of kinetic effects on MHD evolution, and capturing the effects of the MHD relaxation of the profiles within longer time scale transport calculations, requires an integrated simulation. For example, consider the long time scale modeling of a burning plasma configuration. The axisymmetric profiles evolve in response to the turbulent transport and the sources of mass, momentum, and energy from RF antennas and neutral beams, which are in turn affected by the evolution of the profiles. Throughout the simulation the stability of the configuration can be monitored. The stability is affected by the profiles and the presence of the energetic alpha particles that are produced by the fusion reactions. When the configuration becomes unstable it can be used as the initial conditions for an extended MHD simulation. This model would predict the dynamics of the three-dimensional magnetic perturbations and determine their effect on the underlying profiles. In a burning plasma, this calculation would require integrated models for majority ion and electron damping, and for minority (alpha particle) dynamics. The resulting modified profiles could then be returned to the transport calculation for further evolution.

To make progress on this Focused Integration Initiative would require the talents of theoretical and computational plasmas physicists, applied mathematicians, and computer scientists. The existing Extended MHD codes need to be enhanced to include higher resolution and a more rigorous mathematical framework for coupling MHD events with both microscopic effects and with long timescale evolution of profiles, eventually including such effects as plasma rotation and edge effects. The applied math community will be called upon to provide novel methods to deal with the time and spatial scale separation and with the extreme anisotropy; for example moving or adaptive grids, high-order or spectral elements, and nonlinear equation solvers. Since there is no agreed upon “best” method for solution of the Extended MHD equations or for the couplings, there is a need for a computational framework that allows rapid prototyping. Many of the problems faced by this initiative are generic to the larger integration problem. Indeed, since MHD phenomena are intermediate between very fast and very slow phenomena, this FII is a microcosm of the entire project.

D. WHOLE DEVICE MODELING

The distinguishing feature of the Whole-Device Modeling (WDM) FII is that from the outset it will provide a model of the entire device for the whole discharge timescale. Because of this scope, many of the models of individual systems are necessarily very simple. It is envisioned that these simple models will be capable of being replaced by more complete and accurate models as they become available and as is warranted by the application.

The state-of-the-art of whole-device complete-shot modeling at present is represented by the national array of 1-1/2-D transport codes described in Secs. VI and VIII. Those codes have many features that would be required for a final product WDM. They employ a formal separation of time-scales between the rapid (Alfvén) time on which 2-D magnetic equilibria are established, and the much slower time on which heat, particles, and angular momentum, are transported as 1-D surface functions across the magnetic surfaces. They also incorporate many features of a WDM: a hierarchy of models to describe particular aspects of physics, with trade-offs between speed and accuracy; connection to experimental databases; predictive and interpretive modes. Some are also equipped with sophisticated user interfaces.

There are at least three distinct thrusts in a WDM FII. The first is to extend the accuracy and reach of the physics modules available in the existing codes; the second is to extend these codes to fully 3-D geometry so they are applicable to stellarators; and the third is the development of a suitable modern computing framework architecture that would allow this effort to couple to the fruits of the other FIIs for the final WDM code.

The first of these involves the development and application of algorithms for coupling “best physics” modules to the surface-averaged long-timescale transport equations described in Sec. VI. The scientific goals of such couplings are many and diverse: the accurate prediction of heating, fueling, current drive, and confinement on the transport timescale; the ability to account accurately for sawteeth, tearing, and wall modes, in order to assess, avoid, or control them; increased understanding of the complex interaction between the plasma edge and core confinement; and the ability to model and develop machine feedback and control systems within a simulation code environment. Many of these capabilities exist already at some level, and this

activity can be viewed as extending these and taking them to the next level. Extensions would include incorporating rotation and non-Maxwellian distributions into the equilibrium, and self-consistently incorporating multiple heating and current-drive systems into the formulation.

The second major thrust involves coupling 3-D plasma equilibria and device geometry to 1-D surface-averaged transport and the many source and boundary modules that make up a Whole Device Modeling code. This can be viewed as an extension of the present 2-D equilibria + 1-D surface-averaged transport codes, but it is a non-trivial extension. The calculation of 3-D equilibrium is itself a research topic, and issues of existence of surfaces, magnetic islands, and field line stochasticity must be dealt with on both a fundamental mathematical and a practical computational level. It will also be necessary to extend current methods to include plasma rotation and other non-ideal effects. Developing a system to define the complex 3-D input geometry and to manage the extensive output is itself a challenge.

The third major goal of a WDM FII is the design of the code architecture for the final WDM product. This is obviously critical in many respects. Although it may not speed science results within the five-year timeframe of the FIIs, it is important for the success of the global initiative that the framework itself gets a timely start. This thrust, in particular, will rely heavily on computer scientists to develop an extensible framework that meets the many needs of the projects.

By its nature, WDM is an integrated activity, and initiatives in this area will overlap other FIIs. While development and testing of particular couplings will be carried out as narrowly focused projects in the other FIIs, integration into a WDM code is a practical requirement for a close connection to experiment, or for an ability to simulate a proposed new machine on transport timescales. It is also possible for a WDM code to serve as the 1-D transport solver throughout the development of any of the new couplings. This suggests coordinating the WDM FII closely with the turbulence, the MHD, and the edge FIIs.

X. VALIDATION REQUIREMENTS IN FUSION TOPICAL AREAS

What follows are examples of phenomena that one could anticipate being important for validation tests of fusion simulation codes in various topical areas, with particular regard to possible Focused Integration new capabilities. This is not a statement of the outstanding physics issues - but a list of some calculable and measurable (at least in principle) quantities that are important for testing. They are described beginning with the most general and global to the most detailed and local and most stringent. This ordering also reflects the difficulty in making such measurements.

A. TRANSPORT

The coarsest level of agreement between a transport simulation and an experiment would be to match the total stored energy given the input power and other machine parameters. This is only an interesting comparison if the model has few if any free parameters that have been calibrated against existing databases. One should not expect the scaling laws themselves to be derivable as

the engineering parameters used are only proxies for the relevant physics variables. A higher level of agreement could be assessed by comparison of profiles given fluxes or models for the sources. At a minimum, one is interested in the width and height (or gradient) of the edge pedestal and core temperature gradients. Eventually this comparison must be extended to all transport channels, ion and electron thermal, particle (including impurities) and momentum transport. Recent work by ITER expert groups have shown however that a wide range of codes, based on physical, semi-empirical, or wholly empirical models can achieve essentially identical performance in matching temperature profiles for a moderately large set of discharges from a variety of machines. This suggests that agreement at this level is insufficient to validate a particular code. More challenging are comparisons of transient behavior including thresholds and dynamics of transport barriers. Many widely observed features of transient transport cannot be explained by the current generation of models. Ultimately, transport models **must** be validated at the level of turbulence and turbulence dynamics - comparisons that will be paced by the development and deployment of fluctuation diagnostics and analysis techniques. Adding to the difficulties is the prediction that fluctuations vary significantly over the poloidal cross section. Synthetic diagnostics, numerical analogies to the experimental diagnostics need to be developed and adapted to simulation code outputs.

B. MHD

The first test of MHD codes is their ability to reproduce experimental stability limits or operational boundaries for ideal and resistive instabilities, including kinks and ballooning modes, edge localized modes (ELMs) and other edge relaxation phenomena, and resistive wall modes. Especially interesting are modification to the stability boundaries from non-ideal or non-linear effects. A second parameter for comparison is the growth rates of unstable modes, first in their linear phase then in the non-linear phases including the calculation of the saturation levels for these modes. More generally one can look for agreement with the computed eigenvectors and eigenvalues including non-linear mode structures. For example, one should be able to predict various ELM types and their non-linear extent. Large-scale dynamics of disruptions can be compared including halo and eddy current distributions in real machine geometry, runaway populations and so forth. Dedicated experiments should also test explicitly the extensions to ideal MHD including neoclassical, two-fluid, flow, finite Larmor radius and other kinetic effects and non-linear interactions with profiles and transport.

C. RADIO-FREQUENCY HEATING AND CURRENT DRIVE

Validation of RF models is challenging, as the important quantities are particularly difficult to measure. Testing begins with global quantities like overall heating and current drive efficiencies and proceeds to comparisons with deposition profiles for heat, current, and flow velocity. Beyond these measures, an essential element is the verification of RF waves inside the plasmas. To the extent possible, the two-dimensional fields of wave amplitude and wave number should be measured and compared to code predictions. The position of mode conversion layers should be verified along with the propagation of the outgoing waves. Antenna/edge-plasma interactions and the influence of plasma fluctuations on launched waves will challenge both simulations and measurements. Finally, one will need to compare codes with experiments that test the models of wave-particle interactions. For this, one would need to measure velocity-space distributions along with the wave fields and plasma profiles.

D. EDGE/SCRAPE-OFF-LAYER/DIVERTOR

Edge modeling involves a wide range of physical effects including those common with the core like transport and MHD as well as neutral dynamics, atomic processes and plasma-material interactions. Fortunately the diagnostic challenge is not quite as severe in the edge plasma as it is in the core. Assessment of edge transport models is similar to that in the core with comparisons involving profile and fluctuation measurements, though with perhaps greater emphasis on poloidal variation. The energy source from the core to the edge is expected to vary strongly around the poloidal circumference leading to predictions of flows and potentials that must be verified. As in the core, profiles from energy, particle, impurity, and momentum transport should all be compared along with the appearance of self-generated flows. Unlike the core, the sources and sinks for particles, including impurities, are not well characterized. The position and processes for these sources needs to be included in models and tested by experiments. Deposition of impurities and co-deposition of hydrogenic species is a particularly important issue for benchmarking. The role of neutrals is complex, affecting all transport channels through both classical and turbulent processes. The computed three-dimensional distribution of neutrals should be verified and the role of various neutral transport mechanisms tested. A basic model for fueling including sources, neutral dynamics, particle transport needs to be developed and compared with experiments. Finally, important interactions with MHD physics in phenomena like ELMs and the tokamak density limit provide particularly stringent tests for integrated models.

XI. BACKGROUND – ORBITS AND INSTABILITY MECHANISMS

Here, we explain some of the basics of plasma motion embodied in Eq. (A-1). For a more complete explanation, one should consult any plasma physics textbook. The basic equation, describing the motion of a charged particle in electric and magnetic fields, reflecting the force term in Eq. (A-1) is

$$m \frac{d\mathbf{v}}{dt} = q(\mathbf{E} + \mathbf{v} \times \mathbf{B}), \quad (\text{A-28})$$

where q is the particle charge. The basic motion in a uniform magnetic field is gyration about the field line with frequency $\omega_c = qB/m$ and radius $\rho_c = v/\omega_c$. Additional forces and non-uniformities produce drifts in a direction perpendicular to both the force and the magnetic field. Thus, an electric field \mathbf{E} or a gradient ∇B perpendicular to \mathbf{B} reduces the orbital radius on one-half cycle and increases it on the other, resulting in

$$\mathbf{v}_E = \frac{\mathbf{E} \times \mathbf{B}}{B^2}, \text{ and } \mathbf{v}_d = \frac{v_{\perp}^2}{2\omega_c} \frac{\mathbf{B} \times \nabla B}{B^2}, \quad (\text{A-29})$$

the $\mathbf{E} \times \mathbf{B}$ drift and the *grad B drift*, respectively. If the magnetic field is curved, a similar expression is obtained for the curvature drift, which is proportional to v_{\parallel}^2 . In addition to these particle drifts there are fluid drifts in confined plasmas (i.e., plasmas with radial density and

temperature gradients), owing to the fact that at any one radius, there are more particles moving in one direction perpendicular to the gradient than in the reverse direction. This yields a net fluid velocity known as the *diamagnetic drift*

$$\mathbf{v}_a^* = \frac{\rho_a v_a \mathbf{B} \times \nabla n_a}{B n_a}, \quad (\text{A-30})$$

where v_a is the thermal velocity of species a . A similar drift proportional to the temperature gradient is also important in the kinetic theory. For the orderings employed in plasma computation, an important feature of all these drifts is that for thermal particles they are smaller than the thermal velocity by a factor $\rho_a/L \ll 1$, where L is a macroscopic length, e.g. of order ρ^* . All plasma waves, instabilities, and transport phenomena are related in some way to these drifts, which are illustrated in Fig. A12.

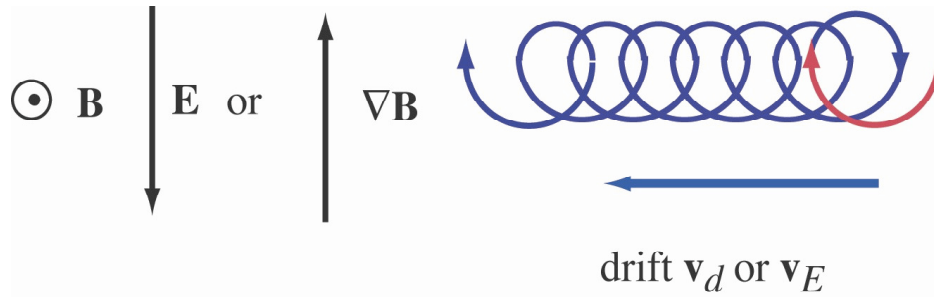


Fig. A12. Ion drifts in electric and magnetic fields.

The existence of waves and instabilities is closely related to the fact that the grad B drift and the diamagnetic drift have opposite signs for ions and electrons (we are taking ρ_a and ω_{ca} to have the sign of q_a), while the $\mathbf{E} \times \mathbf{B}$ drift is the same for each species. For example, Fig. A13 provides a simple picture of instability in *bad curvature*. If a perturbation forms in a region of high pressure gradient, then curvature and grad B drifts cause a charge separation. The resulting electric field drives $\mathbf{E} \times \mathbf{B}$ drifts that amplify the perturbation.

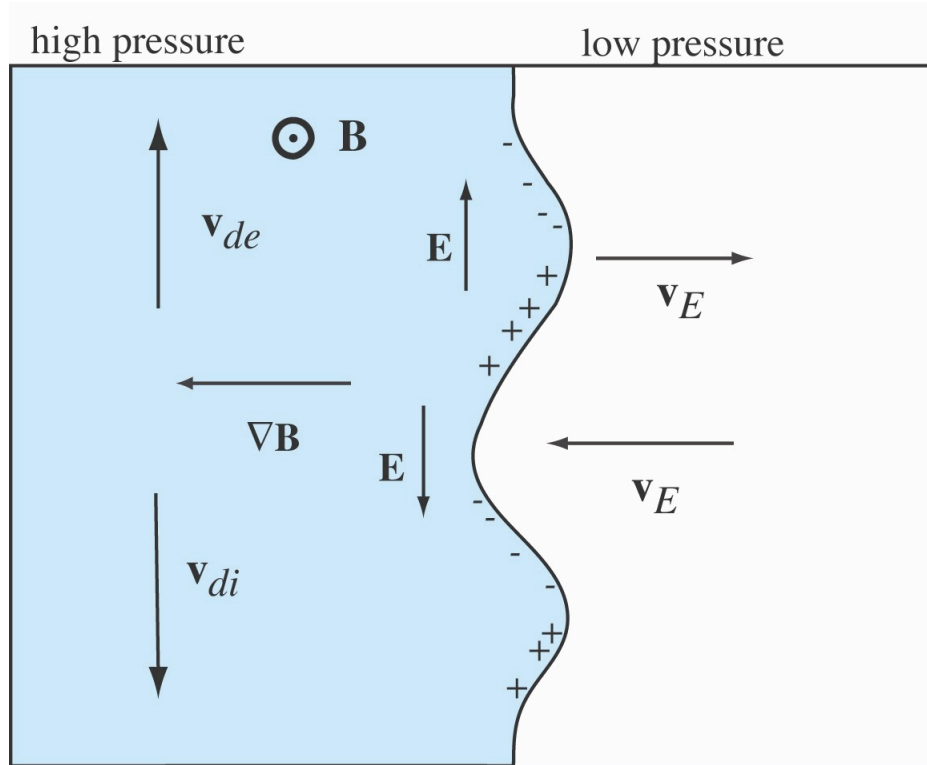


Fig. A13. *Bad curvature instability*

XI. GLOSSARY

Alfvén wave: A plasma wave, which involves bending or compression of the magnetic field. The Alfvén time scale is the interval for an Alfvén wave to traverse the plasma. Magnetosonic waves are a type of Alfvén wave.

Alpha heating: In a fusion power plant, energetic alpha particles and neutrons are created by the fusing of deuterium and tritium nuclei. As a charged particle, the alpha particle is unable to cross the confining magnetic field and gives up its energy as heat to the plasma.

Ambipolarity: Mass transport in plasmas is ambipolar, that is the fluxes of electrons and ions are virtually the same. The densities of negatively and positively charged particles that compose a plasma are almost in perfect balance, leaving the plasma essentially neutral (termed quasi-neutrality).

Aspect ratio: In a toroidal device, the ratio of the major radius to the minor radius.

Avalanche: A sudden macroscopic event in which energy or particles can be distributed across the medium. Often described by simple mathematical models.

Bad curvature: See Curvature.

Ballooning: A local instability, which can develop in the tokamak when the plasma pressure exceeds a critical value. It is analogous to the unstable bulge that develops on an over-inflated pneumatic inner tube.

Banana: The shape of a trapped particle orbit (banana orbit) projected onto a poloidal plane. The shape results from drifts away from a magnetic surface.

Beta: The ratio of plasma pressure to magnetic pressure. An essential dimensionless parameter for magnetized plasmas. Denoted by the symbol β .

Boltzmann equation: An equation of motion in phase space (position and velocity). The Boltzmann equation (and its collisionless version, the Vlasov equation), is the starting point for much of plasma physics and is the fundamental equation for kinetic theory.

Bootstrap current: Currents driven by collisional transport effects in toroidal plasmas (see neoclassical).

Braginskii equations: Plasma fluid equations separately describing electron and ion motion. Fluid equations are obtained by calculating velocity moments of the Boltzmann equation and specifying a closure condition.

Closure: Mathematical scheme by which a hierarchy of equations is truncated. This usually involves expressing higher moments in velocity space in terms of lower moments.

C-Mod: A compact high field tokamak experiment.

Confinement: Property of magnetic fields in preventing loss of energy and particles; degree or measure of this property, as in “confinement time,” for example.

Curvature: In toroidal configurations, field lines are necessarily curved, giving rise to particle drifts. In *bad curvature* or *unfavorable curvature* regions, these drifts give rise to instability (see Fig. A13). In *good curvature* regions, the drifts are stabilizing, owing to the reversal of the relative direction of curvature and pressure gradient. The *grad B drift* acts in a similar way.

Cyclotron frequency: Same as gyrofrequency.

Detached plasma: Cold dense plasma in the divertor chamber, separated from the walls by neutral gas. This is characteristic of a particular mode of divertor operation.

Diamagnetic drifts, waves, etc.: Refers to plasma dynamics driven by the effect of a plasma pressure gradient in a magnetic field.

DIII-D: A medium scale, strongly shaped tokamak experiment.

Disruption: The abrupt termination of a tokamak plasma through the growth of large amplitude MHD instabilities. Control of disruptions is a critical problem for this type of confinement device.

Divertor: Region outside the plasma core with open field lines leading to a chamber some distance from the plasma.

Drift: The motion of a particle or fluid when subjected to a force or gradient perpendicular to the magnetic field. The drift is perpendicular to both the field and the other force. Examples are *curvature drift*, *grad B drift*, *$E \times B$ drift*, and *diamagnetic drift*. See Appendix A8.

Drift wave: A type of plasma wave arising from the presence of density and temperature gradients across magnetic field lines. Turbulence of various types of drift waves is believed to be responsible for anomalous transport in toroidal plasma experiments. *ITG* and *ETG modes* are examples of drift waves.

ECRF: Electron Cyclotron Range of Frequencies – Refers to radio frequency heating and current drive using waves close to the electron cyclotron frequency.

ELM: Edge Localized Mode – a phenomenon that relaxes the pressure gradient of a plasma device operating in H or High confinement mode.

Equilibrium: Usually refers to MHD equilibrium – a steady state solution of the MHD equations. While confined plasmas may be approximately in local thermal equilibrium, they are not in global thermodynamic equilibrium.

ETG: Electron Thermal Gradient (modes) – A type of “micro” plasma instability that may be responsible for turbulent transport by very short (electron cyclotron radius) fluctuations.

Field lines and flux surfaces: Imaginary lines marking the direction of a force field. These map out surfaces (to which plasma particles are approximately constrained) called flux surfaces.

Finite Larmor radius: FLR. A mathematical expansion or approximation in which terms of order the Larmor radius (gyroradius) divided by a macroscopic scale are retained.

FIRE: Fusion Ignition Research Experiment – A proposed burning plasma experiment, which would operate with very high magnetic fields.

FLR: See Finite Larmor radius.

Flux: See Magnetic flux, Transport flux.

Good curvature: See Curvature.

Grad-Shafranov equation: A steady-state MHD equation whose solution yields axisymmetric equilibria.

Gyrofluid: A set of fluid equations that treat ions and electrons separately and retain certain kinetic effects through their closure conditions.

Gyrofrequency: the frequency at which a particle gyrates around a magnetic field line; also called *cyclotron frequency*.

Gyrokinetic: Kinetic equations derived from the Boltzmann equation, which is averaged over the fast cyclotron (gyro) motion of the plasma particles reducing the number of spatial dimensions from 6 to 5.

Gyroradius: the radius at which a particle gyrates about the magnetic field; also called *Larmor radius*.

Hall term: A term in the extended Ohm's law in MHD, proportional to the crossed current and magnetic field. The presence of this term, often neglected in simpler descriptions, leads to whistler waves and can strongly influence the rate of magnetic reconnection.

H-Mode: High (confinement) Mode – an experimental regime with a transport barrier or pedestal at the edge of the plasma.

IBW: See Ion Bernstein Wave.

ICRF: Ion Cyclotron Range of Frequencies - Refers to radio frequency heating, current and flow drive using waves close to the ion cyclotron frequency.

Ion Bernstein Wave (IBW): – short wavelength electrostatic waves in the ion cyclotron range of frequencies. Generated in the plasma by mode conversion.

Ion cyclotron wave: A plasma wave that propagates at frequencies above the ion cyclotron frequency. See ICRF.

IPPA: Integrated Program Planning Activity – the current roadmap for the fusion energy program.

Island – Magnetic Island: A three dimensional magnetic structure arising when closed flux surfaces are perturbed by magnetic fields from plasma fluctuations or from errors in the vacuum fields.

ITB: Internal Transport Barrier – a regime of strongly reduced transport over some part of the core plasma.

ITER: International Thermonuclear Experimental Reactor – A burning plasma experiment proposed as the next step in the international fusion program.

ITG: Ion Thermal Gradient (modes) – A type of “micro” plasma instability that may be responsible for turbulent transport by medium scale (ion cyclotron radius) fluctuations.

JET: Joint European Torus – a large Tokamak experiment run jointly by a European Community consortium.

Kinetic: Refers to aspects of plasma physics related to velocity distributions of electrons and ions.

Kink Instability: A macroscopic (large scale) instability driven by plasma currents.

Larmor radius: Another term for the cyclotron orbit radius of electrons or ions in a magnetic field.

LH: Lower Hybrid – RF waves of frequency intermediate between the electron and ion gyrofrequencies and used for heating and current drive.

L-Mode: Low (confinement) Mode – the baseline for confinement in magnetic fusion devices, dominated by strong turbulent transport.

Lorentz force: The basic electromagnetic force on a particle, $q(\mathbf{E} + \mathbf{v} \times \mathbf{B})$, where q and \mathbf{v} are the particle charge and velocity, and \mathbf{E} and \mathbf{B} are the electric and magnetic fields.

Lundquist number: The ratio of the resistive time scale to the Alfvén time scale. Plays a role for MHD waves analogous to the Reynolds number in fluid dynamics.

Magnetic flux: The integral over a surface area of the magnetic field perpendicular to the surface. Examples are the poloidal flux Ψ and the toroidal flux Φ .

Magnetic surface: A two-dimensional closed toroidal surface on which magnetic field lines lie. In an axisymmetric device, such as a tokamak, the equilibrium consists of nested magnetic surfaces.

Magnetosonic wave: Plasma sound wave, in which the magnetic field is compressed along with the gas.

Major radius: Distance from the center line of the torus to the magnetic axis or center of the plasma cross section.

Maxwellian: Velocity distribution characteristic of local thermal equilibrium: $f \sim \exp(-mv^2/2T)$ where T is the local temperature. (See Equilibrium).

Mercier criterion: A mathematical criterion describing the local stability of MHD modes.

MHD: MagnetoHydroDynamics – A fluid description of magnetized plasmas.

Minor radius: distance from the center of the plasma cross section to the plasma edge.

Mode: 1) a plasma wave that has, at least approximately, constant wavenumber and frequency, or can otherwise be characterized as a normal mode of some wave equation. 2) a mode of operation of a device, such as L-mode or H-mode.

Mode conversion: The process by which waves of one type are converted to another, occurring in a region where the frequency and wavelength of both waves match.

NBI: Neutral Beam Injection – A common method of plasma heating which employs intense beams of neutral atoms.

NCSX: National Compact Stellarator eXperiment – a low aspect-ratio stellarator now in the design phase.

Neoclassical: The theory of collisional transport in toroidal geometry.

NTM: Neoclassical Tearing Modes – Resistive MHD modes driven unstable by bootstrap currents.

Ohmic: Characteristic of dissipation due to plasma resistivity; Ohmic heating, in which a current is driven inductively in the plasma.

Pedestal: Region of steep gradients at plasma edge.

PIC: Particle In Cell – a numerical method for solving kinetic equations by following representative particles moving in self-consistent fields. (Cell refers to the grid used in the computation.)

Poloidal: The short way around in a torus—denoted by θ (see Fig. III.1 of the main report).

Potato: The shape of a particle orbit (potato orbit) close to the magnetic axis – a distorted *banana*, which see.

QPS: Quasi-Poloidal Stellarator: a low aspect-ratio stellarator now in the design phase.

Quasi-linear: In plasma theory, an expansion in powers of wave amplitude in which the fast motion is treated linearly and zero-frequency quadratic terms determine the slow background evolution.

Resonance: 1) A singularity in the electromagnetic plasma wave equations arising from the variation of physical parameters in space. 2) A singularity in the particle distribution function arising from the matching of wave and particle velocities in particular regions of phase space, a wave-particle resonance.

Reynolds Stress: The advection or transport of momentum by turbulence.

RF: Radio Frequency – refers to methods of heating, flow or current drive depending on the interaction of plasmas with externally launched waves.

ρ^* : Pronounced “rho-star”, the ratio of the ion gyroradius to the minor radius. Usually ρ^* is much smaller than unity and is used as an expansion parameter. See Gyrokinetic.

RWM: Resistive wall mode – an MHD mode driven unstable by finite wall resistivity (as opposed to zero resistivity of the ideal MHD theory).

Sawtooth: Sawtooth oscillation, a minor disruption in which core field lines reconnect flattening the temperature profile, followed by a slow reheat of the central plasma. This occurs cyclically.

Self Organized Criticality (SOC): A characteristic of turbulent or chaotic systems where large scale or long lasting structures arise spontaneously and are responsible for significant amounts of transport.

Separatrix: The boundary surface between regions of a plasma on closed and open field lines. Since there is no confinement in the direction parallel to magnetic field lines, the plasma on open field lines is very cold (typically less than a million degrees K).

SOC: See Self Organized Criticality.

SOL: Scrape-Off Layer – region of plasma existing on open field lines outside separatrix.

Stellarator: Unlike most magnetic confinement devices, stellarators employ helical magnetic fields formed by external coils and is intrinsically three-dimensional.

Tearing modes: Resistive MHD modes driven by plasma currents.

TFTR: Tokamak Fusion Test Reactor – a large (former) magnetic confinement experiment.

Tokamak: A magnetic confinement device relying on a large toroidal current carried by the plasma itself. (The acronym is from the Russian phrase TOroidalnaya KAmera i MAgnitnaya Katushka, meaning toroidal chamber and magnetic coil.)

Toroidal: 1) Characteristic of a machine that is shaped like a torus or doughnut. 2) The long way around in a torus-denoted by ϕ (See Fig. III.1 of the main report).

Transport Barrier: Region of strongly reduced transport - typically a bifurcated state. (See ITB, H-mode, and Pedestal).

Transport flux: The total energy or particle flow per unit area passing through a surface element.

Unfavorable curvature: See Curvature.

Vlasov equation: The collisionless version of the Boltzmann equation.

Wave-particle resonance: See Resonance 2).

WDM – Whole Device Modeling

Whistler wave: A high frequency plasma wave with a nonlinear dependence of frequency and wave number. Occurring naturally in the ionosphere, whistler waves were first detected by radio operators during World War I.

X-Point: A point in the plasma cross section where the poloidal magnetic field is zero; occurs at one or more points along the *separatrix*.

Zonal flows: Flows which are constant on flux surfaces but with strong radial variation. These flows are self-generated by plasma turbulence for which it is also an important non-linear saturation mechanism.

FRONT COVER ATTRIBUTION LIST

(APPEARS ON BACK COVER)

*B. Carreras, W. Dorland, L. Garcia
G. Hammett, G. Kerbel, C. Kim
J-N. Leboeuf, V. Lynch, W. Park
S. Parker, B. Rogers, C. Sovinec
D. Spong, R. Sydora, NCSX Team
W7-X Team*